promoter of *CYP1A1*, is also required for the induction of *CYP1A1* [25].

Chromatin remodeling is initiated by liganded AhR/Arnt heterodimer binding to the XREs in the enhancer region, and this leads to increased DNAase sensitivity and the appearance of a DNAase hypersensitive site within 300 bp upstream of the transcription initiation site. BRG1, a component of the SWI/SNF ATP-dependent chromatin-modeling complex, is involved in the TCDD-dependent remodeling of the *CYP1A1* gene [26]. The AhR/Arnt heterodimer transactivates in conjunction with general transcription factors (GTFs) through interactions with coactivator proteins including CBP/p300, SRC-1, NCoA-2 and p/CIP, and the coactivator/corepressor protein RIP140 [27]. In addition, the TRAP/DRIP/ARC/Mediator complex must be recruited to the *CYP1A1* promoter to activate target gene expression in response to xenobiotic stress [28]. However, less is known about the factors regulating the induction of CYP1A2 expression, although the AhR/Arnt heterodimer is clearly required for this to occur. One study suggests that the AhR/Arnt heterodimer may function as a coactivator without directly binding the XRE. Instead, it may interact with other DNA-binding factors of a novel xenobiotic responsive element termed XREII to induce transcription activation [29].

The AhR repressor (AhRR) was identified as a negative regulator of AhR activity. AhRR contains both NLS and NES that are homologous to AhR (Fig. 1b), but AhRR is localized constitutively to the nucleus. Here, AhRR forms a heterodimer with Arnt, but XRE binding by the AhRR/Arnt heterodimer leads to transcriptional repression. Finally, AhRR expression is induced in an AhR-dependent manner, indicating that AhR and AhRR form a regulatory feedback loop [30] (Fig. 2).

Regulation of AhR protein stability

AhR is rapidly degraded both *in vivo* and *in vitro* following ligand binding, and several studies have examined the regulation of AhR degradation. When AhR was fused to the heterologous NLS of nucleoplasmin, it constitutively accumulated in the nucleus and was degraded in a 26S proteasome-dependent manner [31]. Conversely, when nuclear export of AhR was blocked by LMB, AhR accumulated in the nucleus following ligand binding and was not efficiently degraded. In this system, AhR degradation required both an NES and redistribution from the nucleus to the cytoplasm [32]. Although these data are hard to reconcile, a detailed understanding of the factors controlling the degradation of AhR is essential because this is an important component regulating AhR activity. Additionally, it is important to determine whether degradation of AhR is coordinated with cycles of transcriptional activation.

Functional role of AhR in physiology and toxicology

Over the past decade, many studies have examined AhR as a mediator of the adverse cellular response to environmental contaminants, such as TCDD and 3MC. However, the high degree of evolutionary conservation of AhR across a variety of animal species suggests AhR may possess xenobiotic-independent functions [33]. Indeed, a role

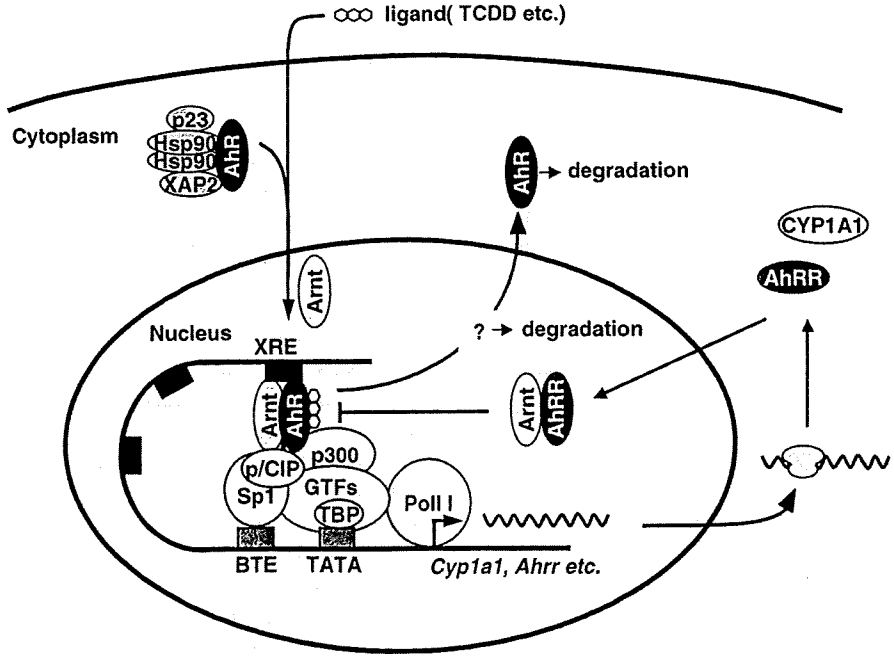

Fig. 2. A model of AhR signaling pathway [5].

for AhR in development was proposed based on the observed expression of AhR and Arnt during mouse embryogenesis [34]. In addition, activation of AhR has been linked to alterations in cell proliferation, apoptosis, adipose differentiation, tumor promotion, and immune and reproductive function. Consistent with these roles, several endogenous compounds, such as bilirubin [35], lipoxin A4 [36] and tryptophan derivatives including FICZ [37], have been isolated as potential natural ligands for AhR. Finally, the generation of AhR-null mice by three independent groups [38–40] has provided strong support for a variety of physiologic roles of AhR, e.g., homeostasis and development.

The role of AhR in carcinogenesis and teratogenesis

A number of papers have examined the role of AhR in regulating the cell cycle and proliferation. However, this remains controversial because studies have reached apparent conflicting conclusions as to whether AhR inhibits or promotes cell cycle progression. One recent report showed that AhR inhibited the growth of epithelial MCF-7 cells, but it promoted the proliferation of HepG2 hepatoma cells. Thus, the precise function of AhR in cell proliferation may differ in a cell type-dependent manner [41]. The constitutive expression of AhR induced tumors in the glandular part of the stomach [42] and increased hepatocarcinogenesis in transgenic B6C3F1 mice following a single injection of *N*-nitrosodiethylamine [43]. Thus, AhR may be oncogenic to varying degrees in different tissues. Consistent with this, AhR-null mice are resistant to benzo[*a*]pyrene-induced tumors [44], directly implicating AhR as a key factor in the development of environmental carcinogenesis. However, the role of AhR in the development of naturally occurring tumors remains largely unknown. In contrast, we recently identified a novel function for AhR as a tumor suppressor in colorectal carcinogenesis (manuscript in preparation).

A role for AhR in renal development has clearly been established. In wild-type mice, exposure to TCDD during development induces hydronephrosis, reduced kidney size, and some developmental renal disorders. In contrast, AhR-deficient mice are completely resistant to these TCDD-induced teratogenic effects [45]. Additionally, in humans with Wilms tumor, a form of renal cancer, there is a relatively high rate of loss of heterozygosity (LOH) at band 7p15-21. A minimal common region of LOH is located between markers *D7S517* and *D7S503* [46], and homozygous deletion of this region is frequently found in these tumors [47]. Interestingly, the *AhR* gene maps to this deleted region, suggesting that AhR may be a candidate for a Wilms tumor suppressor gene. Additionally, a recent paper showed that promoter hypermethylation is a novel epigenetic mechanism downregulating AhR activity in hematological malignancies such as ALL, and, in the patients studied, 33% exhibited some degree of AhR promoter hypermethylation [48].

The role of AhR in reproduction and vascular development

The fertility of AhR-null females is reduced, and the phenotype of these mice is similar to that seen with ARKO and ERα/ERβ double knockout mice. The litter size of AhR deficient mice was significantly decreased compared to wild-type mice [49], and this resulted from impaired folliculogenesis and ovulation in AhR deficient females [50]. An *in vitro* reporter gene assay and *in vivo* ChIP assay suggested that AhR synergistically cooperates with the orphan nuclear receptor Ad4BP/SF-1 to activate *CYP19* gene transcription in ovarian granulosa cells. CYP19 is thought to modulate ovarian estradiol concentrations and drive the estrus cycle. Thus, AhR plays a crucial role in female reproduction by regulating the expression of the ovarian P450 aromatase (CYP19), a key enzyme in estrogen synthesis.

Bradfield et al. [51,52] used a Cre-lox system to study AhR signaling in endothelial/hematopoietic cells, and AhR is necessary for the normal developmental closure of the ductus venosus. In mice unable to express AhR in hepatocytes, the patent ductus venosus results in massive portosystemic shunting of blood flow leading to a profound reduction in hepatocyte size. Although these studies clearly identified an important role for AhR in vascular development, the mechanisms of AhR action in this process remain largely unknown.

The role of AhR in inflammation and the immune system

Environmental exposure to polycyclic hydrocarbons (PAHs) may promote inflammatory and/or allergic disorders, and a role for AhR in inflammation has been suggested. Mice specifically expressing the constitutively active form of AhR (CA-AhR) in keratinocytes appeared normal at birth, but they developed severe skin lesions postnatally. These lesions histologically resembled atopic dermatitis, suggesting that the constitutive activation of the AhR signaling pathway is sufficient to trigger inflammatory skin lesions [53]. In contrast, lipoxins are eicosanoids with potent anti-inflammatory effects in many inflammatory diseases. Lipoxin A4 is a natural ligand for AhR, and it controls the migration of dendritic cells and production of interleukin-12 *in vivo*. Lipoxin A4 activates AhR and increases the expression of suppressor of cytokine signaling 2 (SOCS-2) [54]. Thus, the overwhelming activation of AhR may lead to dysregulated inflammation, but, under normal circumstances, AhR may play an anti-inflammatory role. Further studies are needed to clarify the molecular role of AhR in modulating inflammation.

Thymocyte development and T cell-dependent immune reactions are exquisitely sensitive to AhR-dependent TCDD toxicity. To better understand the role of AhR in T cell development and homeostasis, mice were generated transgenically expressing CA-AhR in T cells under the control of the CD2 promoter. AhR activation in T-lineage cells alone directly induced the thymocyte changes, and the

normal increase in splenocyte number following immunization did not occur in these mice. However, the number of resting splenocytes was not affected, suggesting that AhR functions in the growth of activated and proliferating T cells [55].

Using the B6-into-B6D2F1 model of acute graft-vs.-host disease, Kerkvliet et al. [56,57] showed that AhR activation in donor T cells generates a subpopulation of $CD4^+$ $CD25^+$hi T regulatory cells. They suggested that TCDD-mediated AhR activation preferentially activated these regulatory T cells which subsequently dampened the post-immunization T cell proliferation.

M50367, an orally active anti-allergy agent, is a ligand for AhR, and M50367 activation of AhR signaling skews the Th1/Th2 balance toward Th1 dominance, resulting in immunological responses with anti-allergic effects. This is completely abolished in AhR-null mice. Additionally, forced expression of a constitutively active form of AhR suppresses naïve Th cell differentiation into Th2 cells, demonstrating that AhR functions as a modulator of the *in vivo* Th1/Th2 balance through activation of AhR in naïve Th cells [58].

Taken together, these results suggest that AhR is intimately involved in a number of different aspects of immunological responses. The molecular mechanisms controlling AhR function in the immune system will be interesting to determine in future studies.

Conclusion

CYP1A1 is strongly induced by exogenous ligands such as TCDD, and a number of studies have examined the transcription factors and chromatin remodeling factors responsible for CYP1A1 induction. The genetic regulation of CYP1A1 expression is a good model system for the examination of the temporal and spatial recruitment of various transcription factors, nucleosomal remodeling factors and their interactions. Identifying the physiological functions of AhR, and clarifying the mechanisms responsible for its activation in both normal physiology and in response to xenobiotics will provide great insight into a variety of diverse cellular processes. Additionally, modulation of AhR signaling may be a good candidate for the development of therapies targeting endocrine or environmental diseases.

References

[1] D.R. Nelson, Available from: <http://drnelson.utmem.edu/CytochromeP450.html>.
[2] D.W. Nebert, T.P. Dalton, Nat. Rev. Cancer. 6 (2006) 947–960.
[3] D.J. Waxman, Arch. Biochem. Biophys. 369 (1999) 11–23.
[4] O. Hankinson, Annu. Rev. Pharmacol. Toxicol. 35 (1995) 307–340.
[5] Y. Fujii-Kuriyama, J. Mimura, Biochem. Biophys. Res. Commun. 338 (2005) 311–317.
[6] S.A. Kliewer, B. Goodwin, T.M. Willson, Endocr. Rev. 23 (2002) 687–702.
[7] K. Swales, M. Negishi, Mol. Endocr. 18 (2004) 1589–1598.
[8] U. Savas, K.J. Griffin, E.F. Johnson, Mol. Pharmacol. 56 (1999) 851–857.
[9] T. Ikuta, H. Eguchi, T. Tachibana, Y. Yoneda, K. Kawajiri, J. Biol. Chem. 273 (1998) 2895–2904.
[10] M.K. Bunger, S.M. Moran, E. Glover, T.L. Thomae, G.P. Lahvis, B.C. Lin, C.A. Bradfield, J. Biol. Chem. 278 (2003) 17767–17774.
[11] P. Berg, I. Pongratz, J. Biol. Chem. 276 (2001) 43231–43238.
[12] T. Ikuta, T. Tachibana, J. Watanabe, M. Yoshida, Y. Yoneda, K. Kawajiri, J. Biochem. 127 (2000) 503–509.
[13] A. Kazlauskas, S. Sundstrom, L. Poellinger, I. Pongratz, Mol. Cell. Biol. 21 (2001) 2594–2607.
[14] J.J. LaPres, E. Glover, E.E. Dunham, M.K. Bunger, C.A. Bradfield, J. Biol. Chem. 276 (2000) 6153–6159.
[15] T. Ikuta, J. Watanabe, K. Kawajiri, J. Biochem. 131 (2002) 79–85.
[16] T. Ikuta, Y. Kobayashi, K. Kawajiri, Biochem. Biophys. Res. Commun. 317 (2004) 545–550.
[17] C.M. Sadek, B.L. Allen-Hoffmann, J. Biol. Chem. 269 (1994) 31505–31509.
[18] Y.C. Cho, W. Zheng, C.R. Jefcoate, Toxicol. Appl. Pharm. 199 (2004) 220–238.
[19] T. Ikuta, Y. Kobayashi, K. Kawajiri, J. Biol. Chem. 279 (2004) 19209–19216.
[20] T. Ikuta, K. Kawajiri, Exp. Cell Res. 312 (2006) 3585–3594.
[21] B. Oesch-Bartlomowicz, A. Huelster, O. Wiss, P. Antoniou-Lipfert, C. Dietrich, M. Arand, C. Weiss, E. Bockamp, F. Oesch, Proc. Natl. Acad. Sci. USA 102 (2005) 9218–9223.
[22] N. Dzeletovic, J. McGuire, M. Daujat, J. Tholander, M. Ema, Y. Fujii-Kuriyama, J. Bergman, P. Maurel, L. Poellinger, J. Biol. Chem. 272 (1997) 12705–12713.
[23] M. Backlund, M. Ingelman-Sundberg, Cell Signal. 17 (2005) 39–48.
[24] A. Fujisawa-Sehara, K. Sogawa, M. Yamane, Y. Fujii-Kuriyama, Nucleic Acids Res. 15 (1987) 4179–4191.
[25] A. Kobayashi, K. Sogawa, Y. Fujii-Kuriyama, J. Biol. Chem. 271 (1996) 12310–12316.
[26] S. Wong, O. Hankinson, J. Biol. Chem. 277 (2002) 11821–11827.
[27] T.V. Beischlag, S. Wong, D.W. Rose, J. Torchia, S. Reisz-Porszasz, K. Muhammad, W.E. Nelson, M.R. Probst, M.G. Rosenfeld, O. Hankinson, Mol. Cell. Biol. 22 (2002) 4319–4333.
[28] S. Wong, K. Ge, R.G. Roeder, O. Hankinson, J. Biol. Chem. 279 (2004) 13593–13600.
[29] K. Sogawa, K. Numayama-Tsuruta, T. Takahashi, N. Matsushita, C. Miura, J. Nikawa, O. Gotoh, Y. Kikuchi, Y. Fujii-Kuriyama, Biochem. Biophys. Res. Commun. 318 (2004) 746–755.
[30] J. Mimura, M. Ema, K. Sogawa, Y. Fujii-Kuriyama, Genes Dev. 13 (1999) 20–25.
[31] B.J. Roberts, M.L. Whitelaw, J. Biol. Chem. 274 (1999) 36351–36356.
[32] N.A. Davarinos, R.S. Pollenz, J. Biol. Chem. 274 (1999) 28708–28715.
[33] M.E. Hahn, Chem. Biol. Interact. 141 (2002) 131–160.
[34] B.D. Abbott, L.S. Birnbaum, G.H. Perdew, Dev. Dyn. 204 (1995) 133–143.
[35] J. Adachi, Y. Mori, S. Matsui, H. Takigami, J. Fujino, H. Kitagawa, C.A. Miller, T. Kato, K. Saeki, T. Matsuda, J. Biol. Chem. 276 (2001) 31475–31478.
[36] C.M. Schaldach, J. Riby, L.F. Bjeldanes, Biochemistry 38 (1999) 7594–7600.
[37] Y.D. Wei, H. Hellenberg, U. Rannug, A. Rannug, Chem. Biol. Interact. 110 (1998) 39–55.
[38] P. Fernandez-Salguero, T. Pineau, D.M. Hilbert, T. McPhail, S.S. Lee, S. Kimura, D.W. Nebert, S. Rudihoff, J.M. Ward, F.J. Gonzalez, Science 268 (1995) 722–726.
[39] J.V. Schmidt, G.H. Su, J.K. Reddy, M.C. Simon, C.A. Bradfield, Proc. Natl. Acad. Sci. USA 93 (1996) 6731–6736.
[40] J. Mimura, K. Yamashita, K. Nakamura, M. Morita, T.N. Takagi, K. Nakao, M. Ema, K. Spgawa, M. Yasuda, M. Katsuki, Y. Fujii-Kuriyama, Genes Cells 2 (1997) 645–654.
[41] M. Abdelrahim, R. Smith, S. Safe, Mol. Pharmacol. 63 (2003) 1373–1381.

[42] P. Andersson, J. McGuire, C. Rubio, K. Gradin, M.L. Whitelaw, S. Pettersson, A. Hanberg, L. Poellinger, Proc. Natl. Acad. Sci. USA 99 (2002) 9990–9995.
[43] O. Moennikes, S. Loeppen, A. Buchmann, P. Andersson, C. Ittrich, L. Poellinger, M. Schwarz, Cancer Res. 64 (2004) 4707–4710.
[44] Y. Shimizu, Y. Nakatsuru, M. Ichinose, Y. Takahashi, H. Kume, J. Mimura, Y. Fujii-Kuriyama, Proc. Natl. Acad. Sci. USA 97 (2000) 779–782.
[45] M.H. Falahatpisheh, K.S. Ramos, Oncogene 22 (2003) 2160–2171.
[46] R.G. Grundy, J. Pritchard, P. Scambler, J.K. Cowell, Oncogene 17 (1998) 395–400.
[47] K. Sossey-Alouli, L. Vieira, D. David, M.G. Boavida, J.K. Cowell, Gene. Chromosome. Canc. 36 (2003) 1–6.
[48] S. Mulero-Navarro, J.M. Carvajal-Gonzalez, M. Herranz, E. Ballestar, M.F. Fraga, S. Ropero, M. Esteller, P.M. Fernandez-Salguero, Carcinogenesis 27 (2006) 1099–1104.
[49] B.D. Abbott, J.E. Schmid, J.A. Pitt, A.R. Buckalew, C.R. Wood, G.A. Held, J.J. Diliberto, Toxicol. Appl. Pharmacol. 155 (1999) 62–70.
[50] T. Baba, J. Mimura, N. Nakamura, N. Harada, M. Yamamoto, K. Morohashi, Y. Fujii-Kuriyama, Mol. Cell. Biol. 25 (2005) 10040–10051.
[51] G.P. Lahvis, S.L. Lindell, R.S. Thomas, R.S. McCuskey, C. Murphy, E. Glover, M. Bentz, J. Southard, C.A. Bradfield, Proc. Natl. Acad. Sci. USA 97 (2000) 10442–10447.
[52] J.A. Walisser, E. Glover, K. Pande, A.L. Liss, C.A. Bradfield, Proc. Natl. Acad. Sci. USA 102 (2005) 1758–17863.
[53] M. Tauchi, A. Hida, T. Negishi, F. Katsuoka, S. Noda, J. Mimura, T. Hosoya, A. Yanaka, H. Aburatani, Y. Fujii-Kuriyama, H. Motohashi, M. Yamamoto, Mol. Cell. Biol. 25 (2005) 9360–9368.
[54] F.S. Machado, J.E. Johndrow, L. Esper, A. Dias, A. Bafica, C.N. Serhan, J. Aliberti, Nat. Med. 12 (2006) 330–334.
[55] K. Nohara, X. Pan, S. Tsukumo, A. Hida, T. Ito, H. Nagai, K. Inoue, H. Motohashi, M. Yamamoto, Y. Fujii-Kuriyama, C. Tohyama, J. Immunol. 174 (2005) 2770–2777.
[56] N.I. Kerkvliet, D.M. Shepherd, L. Baecher-Steppan, Toxicol. Appl. Pharmacol. 185 (2002) 146–152.
[57] C.J. Funatake, N.B. Marshall, L.B. Steppan, D.V. Mourich, N.I. Kerkvliet, J. Immunol. 175 (2005) 4184–4188.
[58] T. Negishi, Y. Kato, O. Ooneda, J. Mimura, T. Tanaka, H. Mochizuki, M. Yamamoto, Y. Fujii-Kuriyama, S. Furusako, J. Immunol. 175 (2005) 7348–7356.

nature Vol 446|29 March 2007|doi:10.1038/nature05683

LETTERS

Dioxin receptor is a ligand-dependent E3 ubiquitin ligase

Fumiaki Ohtake[1,2], Atsushi Baba[2], Ichiro Takada[2], Maiko Okada[2], Kei Iwasaki[1], Hiromi Miki[2], Sayuri Takahashi[2,3], Alexander Kouzmenko[1,2], Keiko Nohara[4], Tomoki Chiba[5], Yoshiaki Fujii-Kuriyama[6,7] & Shigeaki Kato[1,2]

Fat-soluble ligands, including sex steroid hormones and environmental toxins, activate ligand-dependent DNA-sequence-specific transcriptional factors that transduce signals through target-gene-selective transcriptional regulation[1]. However, the mechanisms of cellular perception of fat-soluble ligand signals through other target-selective systems remain unclear. The ubiquitin–proteasome system regulates selective protein degradation, in which the E3 ubiquitin ligases determine target specificity[2–4]. Here we characterize a fat-soluble ligand-dependent ubiquitin ligase complex in human cell lines, in which dioxin receptor (AhR)[5–9] is integrated as a component of a novel cullin 4B ubiquitin ligase complex, $CUL4B^{AhR}$. Complex assembly and ubiquitin ligase activity of $CUL4B^{AhR}$ *in vitro* and *in vivo* are dependent on the AhR ligand. In the $CUL4B^{AhR}$ complex, ligand-activated AhR acts as a substrate-specific adaptor component that targets sex steroid receptors for degradation. Thus, our findings uncover a function for AhR as an atypical component of the ubiquitin ligase complex and demonstrate a non-genomic signalling pathway in which fat-soluble ligands regulate target-protein-selective degradation through a ubiquitin ligase complex.

The transcriptional regulatory system and the ubiquitin–proteasome system are two major target-selective systems that control intracellular protein levels. This target selectivity depends on the recognition of specific DNA elements by sequence-specific transcription factors[1] and the recognition of degradation substrates by E3 ubiquitin ligases[2–4]. These transcription factors and ligases serve primarily as specific adaptors that subsequently recruit transcriptional co-regulators and E2 ubiquitin-conjugating enzymes, respectively, to appropriate targets. The selective biological effects of fat-soluble ligands have been reported to be mediated by two classes of sequence-specific transcription factors, nuclear receptors[1] and arylhydrocarbon receptor (AhR) belonging to the basic helix–loop–helix (bHLH)/Per-Arnt-Sim (PAS) family[5–9].

AhR ligands modulate oestrogen and sex hormone, signalling both positively and negatively[8,10–13]. Functional impairments of male and female reproductive organs in AhR-deficient mice indicate the possible importance of AhR in sex hormone signalling[10,14]. Different AhR agonists[9], including 3-methylcholanthrene (3MC) and 2,3,7,8-tetrachlordibenzo-*p*-dioxin (TCDD), modulate oestrogen-dependent oestrogen receptor (ER)-α transactivation through the association of activated AhR/Arnt with ER-α[15]. Similarly, the transcriptional activity of nuclear androgen receptor (AR) was modulated by association with activated AhR (Supplementary Fig. S2a). However, ligand-bound AhR did not block oestrogen-induced co-activator recruitment on the oestrogen-responsive promoter (Supplementary Fig. S2b). This implies another mode of function for ligand-activated AhR beyond transcriptional regulation.

On activation of AhR by 3MC, we observed that protein levels of endogenous ER-α (in mammary tumour MCF-7 cells), ER-β (in ovarian tumour KGN cells) and AR (in prostate cancer LNCaP cells) were drastically decreased (Fig. 1a–c, and Supplementary Fig. 3a) without a change in messenger RNA levels (data not shown), irrespective of the presence of their cognate hormones. Other AhR agonists[9] (namely β-naphthoflavone (β-NF), environmental toxins such as TCDD and benzo[a]pyrene, and the endogenous metabolite indirubin) were similarly effective in protein degradation for ER-α (Fig. 1b) and ER-β/AR (data not shown), in agreement with a previous report on downregulated levels of uterine ER-α protein in rats treated with TCDD[16]. An AhR partial agonist/antagonist α-naphthoflavone (α-NF) was unable to accelerate the degradation of either AhR or ER-α (Fig. 1b, and Supplementary Fig. S3b).

AhR ligand-induced degradation (Fig. 1a–c) and functional repression (Supplementary Fig. S2c, d) of sex steroid receptors were abrogated in the presence of a proteasome inhibitor MG132. Consistently, poly-ubiquitination of ER-α was promoted by the activated AhR regardless of the presence of oestrogen (Fig. 1d, and Supplementary Fig. S3c). Pulse-chase kinetic analysis indicated that 3MC-induced degradation of ER-α was coupled to that of AhR[8,17,18] (Supplementary Fig. S3d). Moreover, the self-ubiquitination activity of the ligand-bound AhR immunocomplex was detected in an E1/E2-dependent manner (Supplementary Fig. S3e). Together with 3MC-dependent recognition of sex steroid receptors by AhR[8,12,13,15], these properties of AhR resemble those of classical adaptor components of the E3 ubiquitin ligase complexes, such as F-box proteins[3] or von Hippel–Lindau protein[19]. We therefore reasoned that activated AhR might act as an E3 ubiquitin ligase complex component.

To address this idea, AhR-containing complexes were purified from HeLa cells expressing Flag–AhR treated with 3MC or α-NF[15,20]. AhR formed large complexes in the presence of 3MC (Supplementary Fig. S4a–c). Further purification revealed five major 3MC-dependent complexes containing AhR (Fig. 1e). Complexes A and C contained well-known co-activators TRAP220/DRIP205/Med220 and p300 (ref. 1) (Supplementary Fig. S4d, e). Endogenous ER-α was detected in complexes B and C; however, ubiquitinated components were seen only in complex B (Fig. 1f, g).

Complex B was composed of the ubiquitin ligase core components cullin 4B (CUL4B)[3,21,22], damaged-DNA-binding protein 1 (DDB1)[23–27] and Rbx1 (Roc1)[3], together with subunits of the proteasomal 19S regulatory particle (19S RP), Arnt and transducin-β-like 3 (TBL3) (Fig. 1h). These components eluted with AhR in the presence of 3MC but not in the presence of α-NF (Fig. 1i, and Supplementary Fig. S4f). Neither CUL4A nor known substrate-specific adaptor components of CUL4A, such as DDB2, CSA and DET1[23,24], were present

[1]ERATO, Japan Science and Technology Agency, 4-1-8 Honcho, Kawaguchi, Saitama 332-0012, Japan. [2]Institute of Molecular and Cellular Biosciences, University of Tokyo, 1-1-1 Yayoi, Bunkyo-ku, Tokyo 113-0032, Japan. [3]Department of Urology, Faculty of Medicine, University of Tokyo, 7-3-1 Hongo, Bunkyo-ku, 113-8655, Japan. [4]National Institute for Environmental Studies, Tsukuba, Ibaraki 305-8506, Japan. [5]Graduate School of Life and Environmental Sciences, and [6]TARA Center, University of Tsukuba, 1-1-1 Tennodai Tsukuba, 305-8577, Japan. [7]SORST, Japan Science and Technology Agency, 4-1-8 Honcho, Kawaguchi, Saitama 332-0012, Japan.

in the AhR–CUL4B complex. As the cullin amino terminus binds adaptor components and the carboxy terminus interacts with an E2 enzyme-binding subunit Rbx1 (ref. 3), we performed tandem purification of the AhR–CUL4B complex with glutathione *S*-transferase (GST)-tagged CUL4B-N (N-terminal domain of CUL4B) and Flag–AhR. This led to the identification of a core complex consisting of five components: DDB1, AhR, Arnt, TBL3 and CUL4B (Fig. 1j). Together with Rbx1, this complex is denoted by $CUL4B^{AhR}$.

Immunoprecipitation of AhR together with endogenous CUL4B from MCF-7 and LNCaP cells was observed only in the presence of 3MC (Fig. 2a, b). Consistently, ligand-dependent co-localization of AhR with CUL4 was seen in MCF-7 cells (Fig. 2c). Whereas CUL4B seemed to act as a scaffold mediating DDB1–TBL3 and AhR–DDB1 interactions in $CUL4B^{AhR}$ (Fig. 2d, lane 4), ligand-activated AhR induced the assembly of complex components (Fig. 2d, lanes 1–3). DDB1 did not bridge CUL4B association with TBL3 or AhR, apparently because of the absence of the signature WDXR/DWD box[22,25–27] of either TBL3 or AhR, which is essential for DDB1 binding (Fig. 2d, lane 5, and Supplementary Fig. S5a). Consistently, specific and 3MC-dependent interaction of the conserved C-terminal acidic domain of AhR with the N-terminal region of CUL4B, but not with DDB1, was observed in a GST pulldown assay (Supplementary Figs S5b and S6). Because a constitutively active AhR mutant (AhRΔPASB)[9] interacted with CUL4B in the absence of ligand (Supplementary Fig. S5b), ligand-dependent structural alteration presumably induces AhR–CUL4B interaction. An AhR mutant lacking the CUL4B-binding

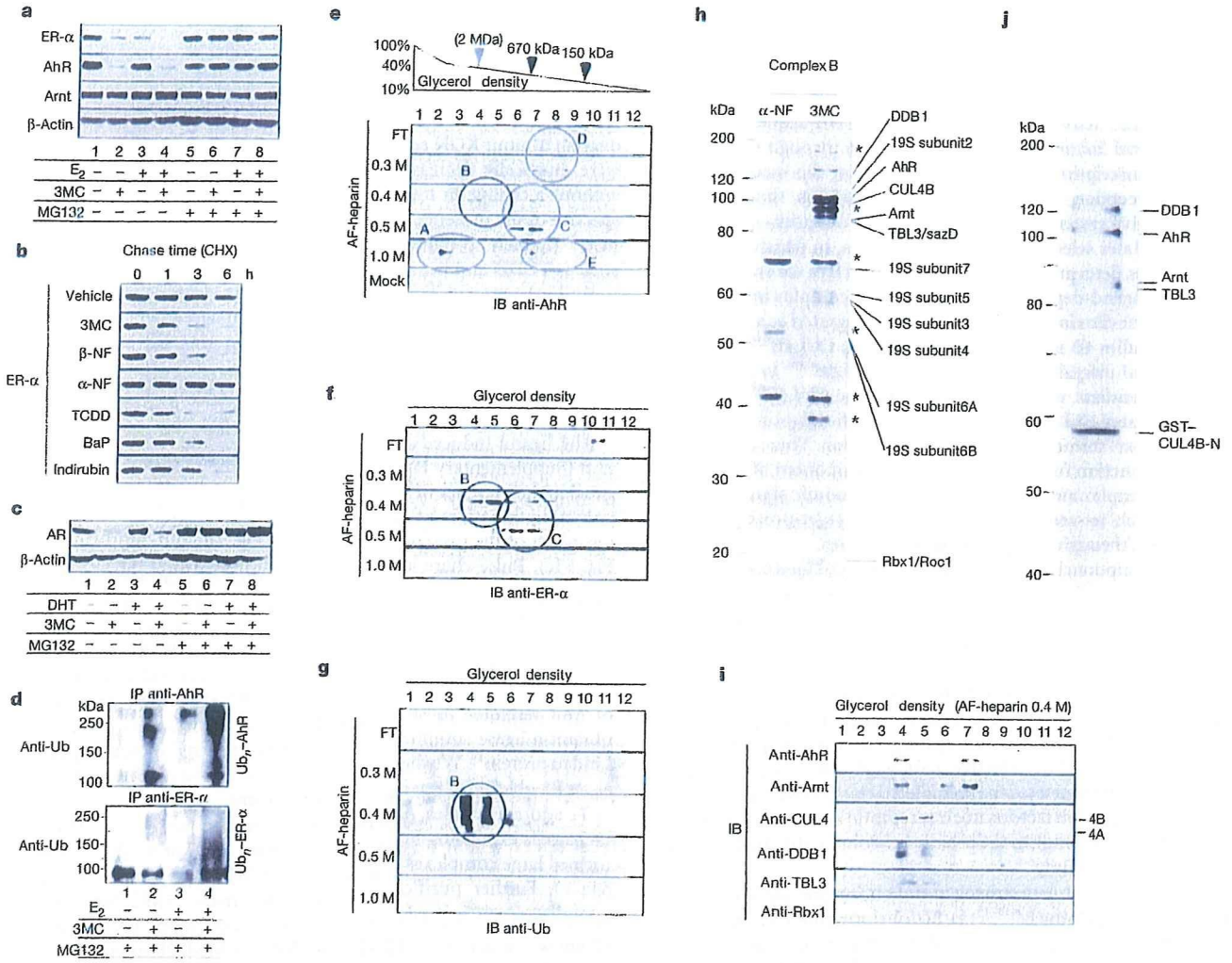

Figure 1 | Activated AhR acts as an E3 ubiquitin ligase. **a–c**, AhR-ligand-induced proteasomal degradation of ER-α (**a**, **b**) and AR (**c**). MCF-7 cells (**a**, **b**) and LNCaP cells (**c**) were incubated as indicated with E_2 (10 nM), DHT (10 nM) and/or 3MC (1 μM), β-NF (1 μM), benzo[a]pyrene (BaP; 100 nM), TCDD (10 nM), indirubin (10 nM) and α-NF (1 μM) in the presence or absence of MG132 (10 μM) and cycloheximide (CHX; 5 μM) for 3 h (**a**, **c**) or the indicated durations (**b**). Cell lysates were subjected to western blotting with specified antibodies. **d**, AhR-ligand-induced ubiquitination of ER-α. MCF-7 cells were incubated with the indicated ligands for 6 h. Western blots were subjected to dark exposure to detect poly-ubiquitinated forms of the receptors. IP, immunoprecipitation; Ub, ubiquitin. **e**, **f**, Biochemical separation and identification of AhR-associated complexes. Flag–AhR-associated proteins in the presence of 3MC or α-NF from HeLa cells stably expressing Flag–AhR were first fractionated by glycerol-density-gradient centrifugation (top, fractions 1–12), and then separated by Toyopearl AF-heparin column chromatography with the indicated KCl concentrations (FT, 1.0 M KCl). Samples from the 3MC-treated cells were resolved into five distinct complexes. IB, immunoblotting. **g**, Components of an AhR-associated complex are highly ubiquitinated. Western blots with anti-ubiquitin antibody. **h**, Identification of AhR-associated CUL4B ubiquitin ligase complex components. Components from complex B in **e** (fractions 4 and 5 from the glycerol-density-gradient centrifugation, eluted from an AF-heparin column at 0.4 M KCl) were resolved by SDS–PAGE, silver-stained and identified by matrix-assisted laser desorption ionization–time-of-flight MS analysis. **i**, Co-elution of the complex B components as a large complex. **j**, Association of activated AhR with the CUL4B complex. The $CUL4B^{AhR}$ complex from Flag–AhR-expressing HeLa cells treated with 3MC was affinity purified with GST-tagged N-terminal domain of CUL4B followed by anti-Flag antibody column fractionation.

acidic domain (AhRΔacid; Supplementary Fig. S6a) was indeed unable to promote ER-α ubiquitination *in vivo*, although the mutant retained 3MC-dependent transactivation function (Supplementary Fig. S5c). This indicates that the ubiquitin ligase function of AhR is independent of its transactivation function.

With two separately prepared components of recombinant AhR and CUL4B/DDB1/Rbx1 purified from *Spodoptera frugiperda* (Sf9) cells (Supplementary Fig. S7a), complex assembly *in vitro* was also dependent on 3MC (Fig. 2e). Furthermore, by *in vitro* ubiquitination assay (Supplementary Fig. S7b), the E3 ubiquitin ligase activity of $CUL4B^{AhR}$ for ER-α was dependent on 3MC but not on 17β-oestradiol (E_2) (Fig. 2f). These data indicate that both the complex assembly and the ubiquitin ligase activity of $CUL4B^{AhR}$ may be dependent on AhR agonists.

We then examined whether the recognition of sex steroid receptors for 3MC-dependent ubiquitination is indeed mediated by AhR. Co-immunoprecipitation analyses indicated that ligand-activated AhR was required for the recruitment of ER-α (Fig. 2a, d) or AR (Fig. 2b, and data not shown) to $CUL4B^{AhR}$. TBL3 and DDB1 did not seem essential for ER-α recruitment but stabilized the association of ER-α with $CUL4B^{AhR}$ (Fig. 2d). Moreover, knockdown of $CUL4B^{AhR}$ components (Supplementary Fig. S8) impaired the 3MC-induced ubiquitination and degradation of ER-α (Fig. 3a–d, and Supplementary Fig. S9a, b) and AR (Fig. 3e, Supplementary Fig. S9c and data not shown), and abolished the AhR-ligand-induced repression of ER-α transactivation (Supplementary Fig. S10a). Recognition of ER-α by activated AhR was retained, but ubiquitination of AhR-bound ER-α was abrogated, by knockdown of the other $CUL4B^{AhR}$ components (Fig. 3d). An ER-α ΔA/B mutant[15] that lacks interaction with AhR, and an ER-α K7R mutant in which seven lysine residues had been replaced with arginine (Supplementary Fig. S6b), were resistant to AhR-dependent ubiquitination and transrepression (Fig. 3f, and Supplementary Fig. S10b). Taken together, these data suggest that ligand-activated AhR functions as a substrate-specific adaptor component of $CUL4B^{AhR}$. AhR is therefore a unique and atypical substrate-specific component of a cullin-based E3 complex, because AhR bears no known interaction motif with cullin complexes yet associates directly with CUL4B. Ubiquitination of ER-α-associated AhR was similarly abolished by the knockdown, and the overall ubiquitination and degradation of AhR[8,17,18] were partly affected (Supplementary Fig. S11a, b). This implies the existence of $CUL4B^{AhR}$-dependent (self-ubiquitination[3]) and $CUL4B^{AhR}$-independent pathways for AhR degradation.

Human ER-α (hER-α) degradation is reportedly accelerated by the binding of E_2 (ref. 1) or the phosphorylation of Ser 118 (ref. 28), whereas a partial antagonist, tamoxifen, has been shown to stabilize ER-α[1]. Nevertheless, 3MC-activated AhR efficiently induced the ubiquitination and subsequent degradation of tamoxifen-bound ER-α and ER-α-S118A mutant (Fig. 3f). Reciprocally, AhR was dispensable for E_2-dependent ER-α degradation (Supplementary Fig. S11c). These results indicate that the $CUL4B^{AhR}$ system may act independently of innate protein degradation system(s) for ER-α. XAP2/ARA9/AIP[7,8,17], a chaperone that modulates the stability of unliganded AhR, seemed unlikely to mediate the accelerated degradation of ER-α by activated AhR (Supplementary Fig. S11d).

Last, we addressed the physiological significance of $CUL4B^{AhR}$ for sex hormone signalling in intact animals. Injection with either 3MC (Fig. 4a) or β-NF (Fig. 4c) did not affect the expression of ER-α or AR mRNA (data not shown) but caused a decrease in protein levels of uterine ER-α in ovariectomized female wild-type mice and of prostate AR in castrated male wild-type mice (Fig. 4b) regardless of their treatment with cognate sex hormones. However, AhR deficiency ($AhR^{-/-}$ mice)[9,14] abolished such effects of AhR ligands but did not affect the modulation of stability of sex steroid receptors by their respective hormones (Fig. 4a, b). As a result of reduced sex steroid receptor levels after pretreatment with 3MC, E_2-dependent induction of c-*fos* in the uterus[15] and dihydrotestosterone (DHT)-dependent induction of *Probasin* in the prostate[10] were severely impaired (Fig. 4a, b). Cellular proliferation and gene induction in response to sex hormones in primary cultured epithelial cells from normal mouse uterus and prostate were consistently suppressed by 3MC (Supplementary Fig. S12a, b) and β-NF (Supplementary Fig. S12c), but no effect was detected in $AhR^{-/-}$ cells (Supplementary Fig. S12a, b). The significance of $CUL4B^{AhR}$ complex components in the AhR-mediated suppression of sex hormone effects

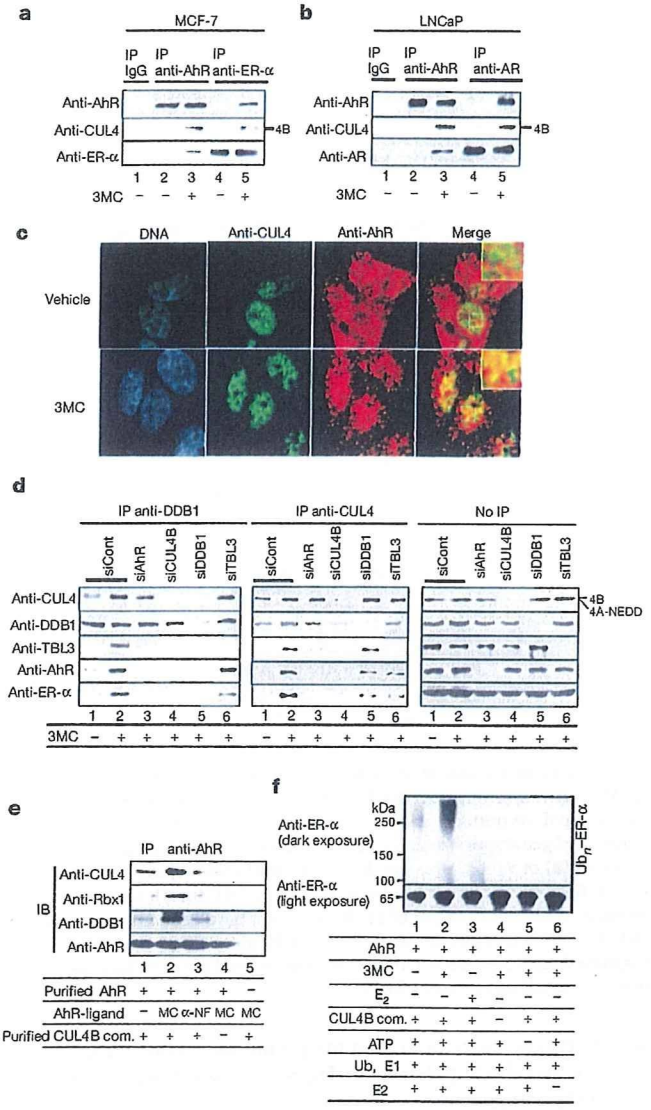

Figure 2 | AhR ligand-dependent assembly and ubiquitin ligase activity of $CUL4B^{AhR}$. **a**, **b**, 3MC-dependent association of endogenous CUL4B and AhR with ER-α and AR. Co-immunoprecipitation analyses from MCF-7 (**a**) and LNCaP (**b**) cells incubated with ligand and MG132 for 2 h. IP, immunoprecipitation. **c**, 3MC-dependent co-localization of AhR with CUL4. MCF-7 cells incubated with 3MC and MG132 for 2 h were immunostained with the indicated antibodies. **d**, Formation of the $CUL4B^{AhR}$ complex. MCF-7 cells were transfected with specified short interfering RNAs (siRNAs) for 48 h, treated with 3MC and MG132 for 2 h, and immunoprecipitated with the indicated antibodies. **e**, Assembly of the CUL4B complex components with AhR is dependent on 3MC *in vitro*. Immunoprecipitation with anti-AhR antibodies of the indicated recombinant CUL4B complex components (CUL4B com.) was observed only in the presence of 3MC. IB, immunoblotting. **f**, $CUL4B^{AhR}$ ubiquitinates ER-α *in vitro*. ER-α protein was incubated with and without recombinant $CUL4B^{AhR}$ E3 complex components, ubiquitin (Ub), ATP, E1 and E2 enzymes as indicated, then subjected to western blotting.

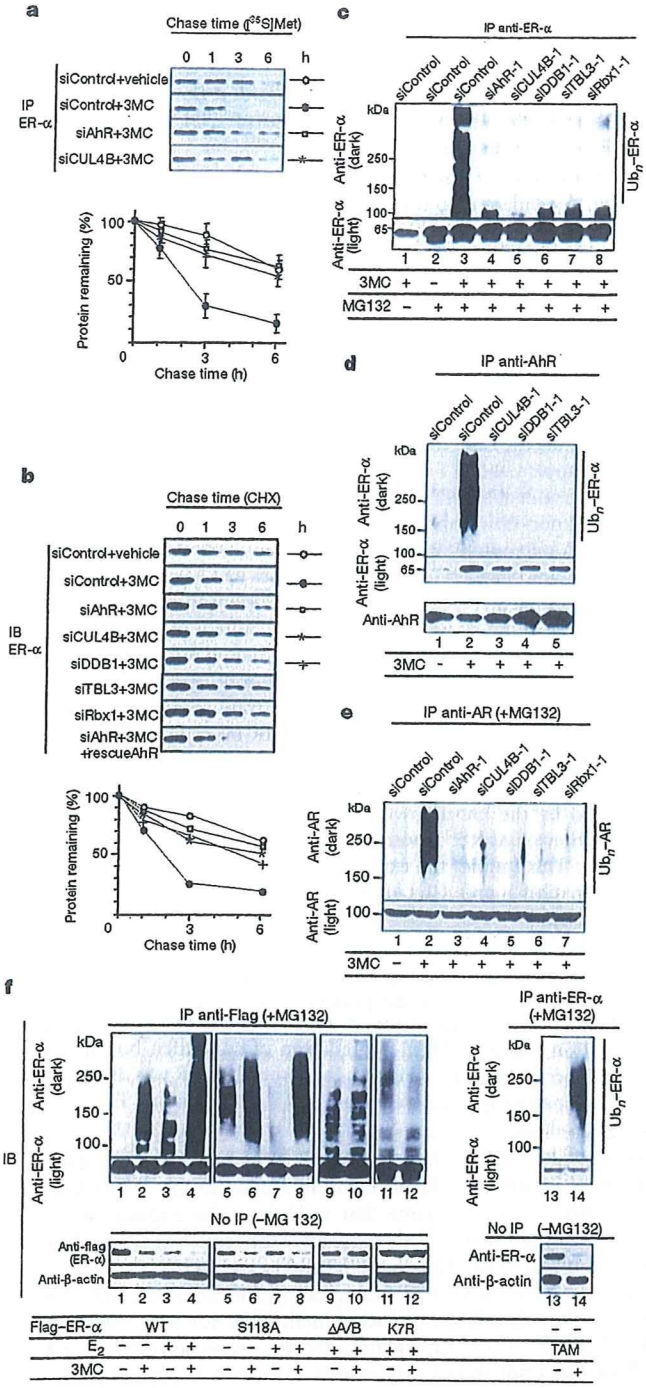

Figure 3 | Activated AhR is a substrate-specific adaptor component of the CUL4B^{AhR} complex. **a–c**, Components of CUL4B^{AhR} are required for 3MC-dependent ubiquitination and degradation of ER-α. MCF-7 cells were transfected with indicated siRNAs for 48 h, then used in pulse-chase analysis as in Supplementary Fig. S3d (**a**), in cycloheximide (CHX) chasing (**b**) and in the *in vivo* ubiquitination assay with ligand incubation for 6 h (**c**). All values are shown as means ± s.d. ($n = 3$) (**a**) or as means ($n = 3$) (**b**). The knockdown efficiency in the same lysates was confirmed in Supplementary Fig. S9a. IB, immunoblotting; IP, immunoprecipitation. **d**, AhR is the substrate-specific adaptor in the targeting of ER-α by CUL4B^{AhR}. MCF-7 cells transfected with the indicated siRNAs were lysed in TNE buffer and immunoprecipitated with anti-AhR antibody in the presence of MG132. Ubiquitination of the ER-α co-immunoprecipitated with AhR was detected by western blotting. **e**, LNCaP cells were subjected to the same analysis as in **a–c**. **f**, AhR-ligand-induced ER-α ubiquitination requires intact lysine

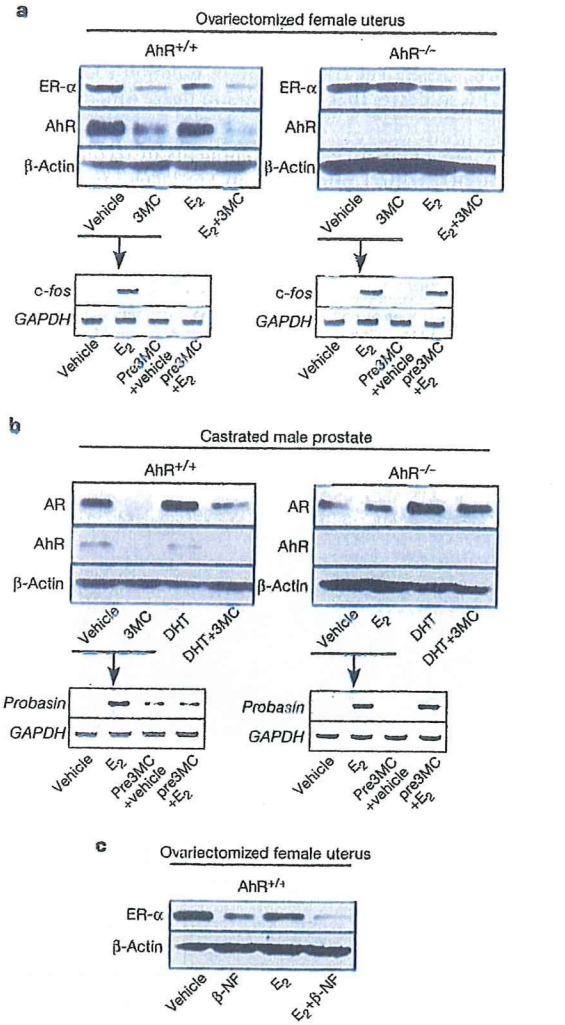

Figure 4 | Ligand-dependent ubiquitin ligase function of AhR *in vivo*. **a, b**, AhR activation enhances the degradation of ER-α and AR *in vivo*. Top: nine-week-old ovariectomized female mice (**a**) or castrated male mice (**b**) of the indicated genotypes were injected with vehicle or indicated ligands. After 4 h, uterus (**a**) or ventral prostate (**b**) was isolated and subjected to western blotting. Bottom: mice pretreated with vehicle or 3MC for 8 h were injected with either vehicle or E_2 (**a**), or DHT (**b**). After 4 h, the uterus or prostate was isolated for reverse transcriptase PCR. GAPDH, glyceraldehyde-3-phosphate dehydrogenase. **c**, Other AhR agonists produce a similar effect on oestrogen signalling to that of 3MC.

(Supplementary Fig. S12a, b) and the promotion of ER-α degradation in uterine cells (Supplementary Fig. S12d) was verified by knockdown of the components.

Here we have shown that a known sequence-specific transcription factor AhR acts as a ligand-dependent CUL4B-based E3 ubiquitin ligase for selectively targeting sex steroid receptors to bring about accelerated protein degradation. The transcription and ubiquitination functions of AhR seem to be responsible for a distinct set of biological events caused by endogenous and exogenous AhR ligands. In ubiquitin ligase complexes, substrate recognition by known

residues and is independent of oestrogen binding or S118 phosphorylation of hER-α. Intact MCF-7 cells (right) or cells transfected with Flag–hER-α, AhR and their derivatives (left) were treated with the indicated ligands in the presence (top) or absence (bottom) of MG132 for 6 h, then subjected to western blotting. TAM, tamoxifen; WT, wild type.

substrate-specific components is generally evoked by substrate modifications[2–4]. However, the recognition and subsequent ubiquitination of sex steroid receptors by AhR requires dioxin-type compounds as ligands but does not require the phosphorylation or ligand binding of sex steroid receptors. We have therefore shown that fat-soluble ligands directly control the function of a ubiquitin ligase complex for targeted protein destruction in animals (see Supplementary Fig. S1). In plants, auxin was recently found to control protein destruction through the auxin receptor SCF^{TIR1} (refs 29, 30). However, whereas SCF^{TIR1} is regulated by ligand-dependent substrate recognition by TIR1, $CUL4B^{AhR}$ is primarily regulated by the assembly of a ligand-dependent complex as well as substrate recognition. Considered together, ubiquitin-ligase-based perception mechanisms of fat-soluble ligands may be diverse in different species. It is possible that other nuclear receptors and binding proteins for fat-soluble ligands also serve as key components of ubiquitin ligases to mediate a non-genomic pathway of fat-soluble ligands to regulate target-protein-selective destruction.

METHODS

More detailed descriptions of all materials and methods are supplied in the Supplementary Information.

Biochemical purification and separation of AhR-associated complexes. The nuclear extracts preparation, anti-Flag affinity purification and mass spectrometry were performed as described previously[15,20]. For purification of the core $CUL4B^{AhR}$ complex, the nuclear extracts were first bound to the GST–CUL4B-N (amino acid residues 1–318) columns before being loaded on anti-Flag columns[20].

***In vitro* ubiquitination assay.** The *in vitro* ubiquitination assay was performed as described previously[23]. Purified Flag–AhR (0.2 μg) was incubated either with 3MC (10 μM) or vehicle (dimethylsulphoxide) for 30 min at 25 °C, then mixed with Flag–CUL4B/DDB1/Rbx1 complex (0.2 μg), and after further incubation for 30 min at 25 °C the substrate, ER-α (Calbiochem), was added.

Plasmids, antibodies, immunoprecipitation, *in vivo* ubiquitination, pulse-chasing, ligand responses in mice, and RNA-mediated interference experiments. Detailed methods used in this study can be found in the Supplementary Information.

Received 13 December 2006; accepted 16 February 2007.

1. McKenna, N. J. & O'Malley, B. W. Combinatorial control of gene expression by nuclear receptors and coregulators. *Cell* 108, 465–474 (2002).
2. Hershko, A. & Ciechanover, A. The ubiquitin system. *Annu. Rev. Biochem.* 67, 425–479 (1998).
3. Deshaies, R. J. SCF and Cullin/Ring H2-based ubiquitin ligases. *Annu. Rev. Cell Dev. Biol.* 15, 435–467 (1999).
4. Harper, J. W. A phosphorylation-driven ubiquitination switch for cell-cycle control. *Trends Cell Biol.* 12, 104–107 (2002).
5. Poellinger, L. Mechanistic aspects—the dioxin (aryl hydrocarbon) receptor. *Food Addit. Contam.* 17, 261–266 (2000).
6. Hankinson, O. The aryl hydrocarbon receptor complex. *Annu. Rev. Pharmacol. Toxicol.* 35, 307–340 (1995).
7. Swanson, H. I. & Bradfield, C. A. The AH-receptor: genetics, structure and function. *Pharmacogenetics* 3, 213–230 (1993).
8. Carlson, D. B. & Perdew, G. H. A dynamic role for the Ah receptor in cell signaling? Insights from a diverse group of Ah receptor interacting proteins. *J. Biochem. Mol. Toxicol.* 16, 317–325 (2002).
9. Mimura, J. & Fujii-Kuriyama, Y. Functional role of AhR in the expression of toxic effects by TCDD. *Biochim. Biophys. Acta* 1619, 263–268 (2003).
10. Lin, T. M. *et al.* Effects of aryl hydrocarbon receptor null mutation and in utero and lactational 2,3,7,8-tetrachlorodibenzo-*p*-dioxin exposure on prostate and seminal vesicle development in C57BL/6 mice. *Toxicol. Sci.* 68, 479–487 (2002).
11. Brunnberg, S. *et al.* The basic helix-loop-helix-PAS protein ARNT functions as a potent coactivator of estrogen receptor-dependent transcription. *Proc. Natl Acad. Sci. USA* 100, 6517–6522 (2003).
12. Matthews, J., Wihlen, B., Thomsen, J. & Gustafsson, J. A. Aryl hydrocarbon receptor-mediated transcription: ligand-dependent recruitment of estrogen receptor α to 2,3,7,8-tetrachlorodibenzo-*p*-dioxin-responsive promoters. *Mol. Cell. Biol.* 25, 5317–5328 (2005).
13. Beischlag, T. V. & Perdew, G. H. ER α-AHR-ARNT protein–protein interactions mediate estradiol-dependent transrepression of dioxin-inducible gene transcription. *J. Biol. Chem.* 280, 21607–21611 (2005).
14. Baba, T. *et al.* Intrinsic function of the aryl hydrocarbon (dioxin) receptor as a key factor in female reproduction. *Mol. Cell. Biol.* 25, 10040–10051 (2005).
15. Ohtake, F. *et al.* Modulation of oestrogen receptor signalling by association with the activated dioxin receptor. *Nature* 423, 545–550 (2003).
16. Romkes, M., Piskorska-Pliszczynska, J. & Safe, S. Effects of 2,3,7,8-tetrachlorodibenzo-*p*-dioxin on hepatic and uterine estrogen receptor levels in rats. *Toxicol. Appl. Pharmacol.* 87, 306–314 (1987).
17. Davarinos, N. A. & Pollenz, R. S. Aryl hydrocarbon receptor imported into the nucleus following ligand binding is rapidly degraded via the cytosplasmic proteasome following nuclear export. *J. Biol. Chem.* 274, 28708–28715 (1999).
18. Roberts, B. J. & Whitelaw, M. L. Degradation of the basic helix-loop-helix/Per-ARNT-Sim homology domain dioxin receptor via the ubiquitin/proteasome pathway. *J. Biol. Chem.* 274, 36351–36356 (1999).
19. Maxwell, P. H. *et al.* The tumour suppressor protein VHL targets hypoxia-inducible factors for oxygen-dependent proteolysis. *Nature* 399, 271–275 (1999).
20. Kitagawa, H. *et al.* The chromatin-remodeling complex WINAC targets a nuclear receptor to promoters and is impaired in Williams syndrome. *Cell* 113, 905–917 (2003).
21. Zhong, W., Feng, H., Santiago, F. E. & Kipreos, E. T. CUL-4 ubiquitin ligase maintains genome stability by restraining DNA-replication licensing. *Nature* 423, 885–889 (2003).
22. Higa, L. A. *et al.* CUL4–DDB1 ubiquitin ligase interacts with multiple WD40-repeat proteins and regulates histone methylation. *Nature Cell Biol.* 8, 1277–1283 (2006).
23. Groisman, R. *et al.* The ubiquitin ligase activity in the DDB2 and CSA complexes is differentially regulated by the COP9 signalosome in response to DNA damage. *Cell* 113, 357–367 (2003).
24. Wertz, I. E. *et al.* Human De-etiolated-1 regulates c-Jun by assembling a CUL4A ubiquitin ligase. *Science* 303, 1371–1374 (2004).
25. Jin, J., Arias, E. E., Chen, J., Harper, J. W. & Walter, J. C. A family of diverse Cul4-Ddb1-interacting proteins includes Cdt2, which is required for S phase destruction of the replication factor Cdt1. *Mol. Cell* 23, 709–721 (2006).
26. Angers, S. *et al.* Molecular architecture and assembly of the DDB1–CUL4A ubiquitin ligase machinery. *Nature* 443, 590–593 (2006).
27. He, Y. J., McCall, C. M., Hu, J., Zeng, Y. & Xiong, Y. DDB1 functions as a linker to recruit receptor WD40 proteins to CUL4–ROC1 ubiquitin ligases. *Genes Dev.* 20, 2949–2954 (2006).
28. Valley, C. C. *et al.* Differential regulation of estrogen-inducible proteolysis and transcription by the estrogen receptor alpha N terminus. *Mol. Cell. Biol.* 25, 5417–5428 (2005).
29. Dharmasiri, N., Dharmasiri, S. & Estelle, M. The F-box protein TIR1 is an auxin receptor. *Nature* 435, 441–445 (2005).
30. Kepinski, S. & Leyser, O. The *Arabidopsis* F-box protein TIR1 is an auxin receptor. *Nature* 435, 446–451 (2005).

Supplementary Information is linked to the online version of the paper at www.nature.com/nature.

Acknowledgements We thank K. Tanaka, C. K. Glass, J. Yanagisawa, Y. Gotoh and J. Mimura for comments; S. Murata, T. Matsuda, T. Suzuki and Y. Tateishi for providing materials; T. Matsumoto, M. Igarashi and S. Fujiyama for technical assistance; and H. Higuchi for manuscript preparation. This work was supported in part by the Program for Promotion of Basic Research Activities for Innovative Biosciences (PROBRAIN) and priority areas from the Ministry of Education, Culture, Sports, Science and Technology (to Y.F.-K. and S.K.).

Author Contributions F.O., T.C., Y.F.-K. and S.K. designed the experiments. F.O., A B., M.O., K I., H.M., S.T. and I. T. performed the experiments. F.O., A.K. and S.K. wrote the paper.

Author Information Reprints and permissions information is available at www.nature.com/reprints. The authors declare no competing financial interests. Correspondence and requests for materials should be addressed to S.K. (uskato@mail.ecc.u-tokyo.ac.jp).

Effects of Environmental Antiandrogenic Chemicals on Expression of Androgen-Responsive Genes in Rat Prostate Lobes

Tomoharu Suzuki,[a] Nariaki Fujimoto,[b] Shigeyuki Kitamura,[c] and Shigeru Ohta*,[a]

[a]*Graduate School of Biomedical Sciences, Hiroshima University,* [b]*Research Institute for Radiation Biology and Medicine, Hiroshima University, 1–2–3, Kasumi, Minami-ku, Hiroshima 734–8551, Japan, and* [c]*Nihon Pharmaceutical University, 10281, Komuro, Inamachi, Kitaadachi-gun, Saitama 362–0806, Japan*

(Received February 6, 2007; Accepted April 9, 2007)

Rat prostate, which is usually used in the Hershberger assay for evaluating the antiandrogenic activity of environmental chemicals *in vivo*, has a complex structure consisting 4 lobes, *i.e.*, the ventral prostate (VP), lateral prostate (LP), dorsal prostate (DP) and anterior prostate (AP). The VP is considered to have no counterpart in primates, while the LP and DP are histologically similar to human prostate. However, the Hershberger assay focuses on the VP, not the other lobes. Moreover, there are few other methods for assessment of antiandrogenic activity *in vivo*. We therefore investigated androgen-responsive genes in the DP, as well as VP, following treatment with environmental chemicals reported to be androgen antagonists. Male castrated F344 rats were treated with testosterone (0.5 $mg \cdot kg^{-1} \cdot day^{-1}$) alone or together with flutamide (6 $mg \cdot kg^{-1} \cdot day^{-1}$) as a reference antiandrogen or fenthion (25 $mg \cdot kg^{-1} \cdot day^{-1}$) or fenitrothion (25 $mg \cdot kg^{-1} \cdot day^{-1}$) or 2,4,4′-trihydroxybenzophenone (2,4,4′-triOH-BP) (300 $mg \cdot kg^{-1} \cdot day^{-1}$) for 7 days. Testosterone significantly increased the expression of kallikrein S3, cystatin-related protein-1 (CRP-1) and prostatein C3 mRNAs in the VP, and prostate secretory protein of 94 amino acids (PSP94) mRNA, but not stem cell growth factor (SCGF) mRNA, in the DP. Coadministration of flutamide blocked the testosterone-induced increases of all three mRNAs in the VP, but not that of PSP94 mRNA in the DP. Coadministration of fenitrothion significantly reduced the testosterone-induced increase of kallikrein S3 mRNA, while fenthion significantly increased the testosterone-induced increase of PSP94 mRNA. 2,4,4′-TriOH-BP significantly increased the testosterone-induced increases of CRP-1 and prostatein C3 mRNAs. These results indicate that the effects of environmental chemicals on the prostate are very complex. The Hershberger assay alone appears to be inadequate for risk assessment, and it may be useful to employ androgen-responsive genes as additional markers.

Key words——antiandrogenic activity, androgen-responsive genes, rat prostate lobes, Hershberger assay, quantitative reverse transcriptase polymerase chain reaction

INTRODUCTION

Many environmental xenobiotics exert hormonal effects at the cellular and organism levels. These compounds are able to mimic the biological activity of sex hormones and thyroid hormone, and are called endocrine-disrupting chemicals. Initially, estrogenic chemicals such as alkylphenols and bisphenol A were discovered,[1,2] while more recently, several environmental pollutants were discovered to be androgen antagonists.[3,4]

*To whom correspondence should be addressed: Graduate School of Biomedical Sciences, Hiroshima University, 1–2–3, Kasumi, Minami-ku, Hiroshima 734–8551, Japan. Tel.: +81-82-257-5325; Fax: +81-82-257-5329; E-mail: sohta@hiroshima-u.ac.jp

The Hershberger assay has been used to detect chemicals with androgen receptor (AR)-mediated activity *in vivo*.[5–7] The advantages of this assay are that is straightforward, quick and relatively specific to androgenic/antiandrogenic compounds. The endpoint of this assay involves weighing the accessory sex organs of castrated male rats treated with an AR agonist and test compounds.[8,9] However, the Hershberger assay is usually focused on the rat ventral prostate (VP), not other lobes. The rat prostate has a complex structure, consisting of a VP, lateral prostate (LP), dorsal prostate (DP) and anterior prostate (AP). The rodent VP is considered to have no counterpart in primates, while the LP and DP are histologically similar to the human prostate.[10]

We recently reported the lobe-specific expres-

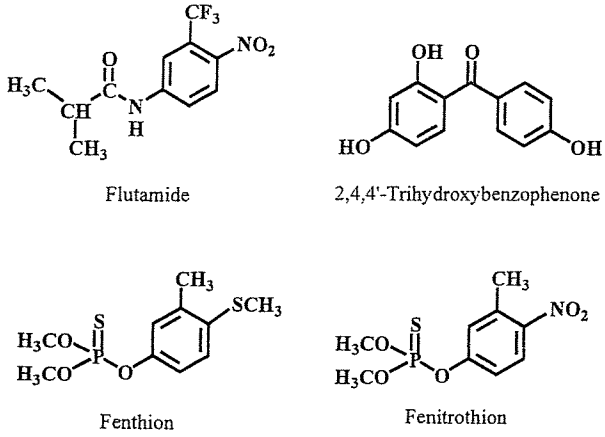

Fig. 1. Structures of Benzophenone, Fenthion and Fenitrothion

sion and lobe-specific response to androgen of several androgen-responsive genes.[11] In the VP, kallikrein S3, cystatin-related protein-1 (CRP-1) and prostatein C3 were highly responsive to androgen treatment. On the other hand, in the LP and DP, prostate secretory protein of 94 amino acids (PSP94), and stem cell growth factor (SCGF) were responsive. In the present study, we used three antiandrogenic chemicals, fenthion, fenitrothion and 2,4,4′-trihydroxybenzophenone (2,4,4′-triOH-BP), as well as the reference antiandrogen flutamide (Fig. 1), and quantitatively analyzed the changes of expression of the above genes in the DP and VP after administration of these chemicals to castrated rats using the same schedule as in the Hershberger assay.[4,12,13] Based on the results, we discuss whether androgen-responsive genes might be suitable markers for assessment of the antiandrogenic activity of environmental chemicals.

MATERIALS AND METHODS

Chemicals —— Testosterone propionate, fenthion and fenitrothion were purchased from Wako Junyaku KK, Osaka, Japan, flutamide from Sigma (St. Louis, MO, U.S.A.) and 2,4,4′-triOH-BP from Tokyo Chemical Industry Co., Ltd., Tokyo, Japan.

Animals —— Animal experiments were conducted according to "A Guide for the Care and Use of Laboratory Animals of Hiroshima University." Male F344 rats were purchased at 4 weeks of age from Charles River Japan Co. (Kanagawa, Japan) and maintained with free access to basal diet and tap water. All animals were surgically castrated at 5 weeks old. At the age of 7 weeks, they were divided into 6 groups each consisting of 6 animals. The rats were treated once a day for 7 days with subcutaneous doses of 0.3 ml of vehicle (dimethyl sulfoxide), testosterone propionate (0.5 $mg \cdot kg^{-1} \cdot day^{-1}$), testosterone propionate plus flutamide (6 $mg \cdot kg^{-1} \cdot day^{-1}$), testosterone propionate plus fenitrothion (25 $mg \cdot kg^{-1} \cdot day^{-1}$), testosterone propionate plus fenthion (25 $mg \cdot kg^{-1} \cdot day^{-1}$) or testosterone propionate plus 2,4,4′-triOH-BP (300 $mg \cdot kg^{-1} \cdot day^{-1}$). Animals were sacrificed under anesthesia and the prostate and seminal vesicles were removed, immediately frozen in liquid nitrogen, and stored at −80 °C.

Quantification of mRNAs by Real-time RT-PCR —— RNA preparation was carried out with a Total RNA Isolation kit (Promega Co., Madison, WI, U.S.A.). Total RNA (2 μg) was reverse-transcribed with 200 U of MMLV-RT (Invitrogen Corp., Carlsbad, CA, U.S.A.) and 2.5 pmol of oligo-dT primer (Invitrogen) in 25 μl of buffer containing 1 mM dNTP, 100 mM Tris–HCl (pH 8.3), 150 mM KCl, 6 mM $MgCl_2$, 60 mM dithiothreitol and 5 U/μl RNasin with incubation at 37 °C for 60 min. A real-time PCR method with a QuantiTect Sybr Green PCR kit (Qiagen, Valencia, CA, U.S.A.) and an ABI Prism 7700 (PerkinElmer Life Sciences, Boston, MA, U.S.A.) was employed for quantitative measurement, following the supplied protocol.[14] Specific primer sets with a Tm of about 59 °C were designed for each mRNA (Table 1). The PCR conditions were 15 min of initial activation followed by 45 cycles of 20 sec at 94 °C, and 30 sec at 58 °C and 40 sec at 72 °C. Prior to quantitative analysis, PCR products were prepared separately and purified by gel-electrophoresis. Extracted fragments were used as standards for quantification. The DNA sequences were confirmed with a capillary DNA sequencer, ABI 310 (PerkinElmer Life Sciences). All mRNA contents were normalized with reference to β-actin mRNA.

Statistical Analysis —— Statistical comparisons were made using ANOVA followed by Scheffe's test.

RESULTS

Effects of Test Chemicals on mRNA Expression of Androgen-responsive Genes

In order to evaluate the effects of several environmental chemicals on the expression of androgen-

Table 1. Primers for Quantitative PCR of Rat Genes

Gene	GenBank Acc#	5′-Primer	3′-Primer
kallikrein S3	M11566	5′-AATTCCCAACCCTGGCAAGT-3′	5′-CGCTGAGCAAAGGGTTCATC-3′
CRP-1	S57980	5′-TGCTCCTACTGGCCATCTTTG-3′	5′-TGTCAGCACTGTGCGTGTTG-3′
prostatein C3	M71245	5′-CAGTGGTTCTGGCTGCAGTATT-3′	5′-CTAGAAAACACTGCTTGAATTGCTTC-3′
PSP94	U65486	5′-GATCACCTGCTGCACCAAAAC-3′	5′-TTCCTGGGTTCGTCCGTTC-3′
SCGF	XM_218611	5′-AGAGGAAACCACCACAACACCT-3′	5′-GTCCAAAACATGCAGACGGAT-3′
β-actin	X03765	5′-CTGTCCCTGTATGCCTCTGGTC-3′	5′-TGAGGTAGTCCGTCAGGTCCC-3′

Table 2. mRNA Levels Expressed by Reportedly Androgen-sensitive Genes in Castrated Rats in the Experimental Treatment Groups

Treatment group	VP			DP	
	Kallikrein S3 mRNA	CRP-1 mRNA	Prostatein C3 mRNA	PSP94 mRNA	SCGF mRNA
Vehicle Control	0.003 ± 0.0002**	0.0004 ± 0.0002**	0.02 ± 0.005**	1.3 ± 0.32**	0.018 ± 0.003
T	7.3 ± 1.1	46 ± 9.0	84 ± 4.1	11 ± 2.0	0.028 ± 0.010
T+Flu	0.060 ± 0.016**	0.30 ± 0.010**	6.4 ± 1.7**	8.7 ± 1.2	0.022 ± 0.002
T+MPP	5.5 ± 0.70	40 ± 4.8	86 ± 10	19 ± 2.2*	0.045 ± 0.011
T+MEP	4.0 ± 0.66*	23 ± 3.1	84 ± 14	15 ± 2.1	0.028 ± 0.003
T+2,4,4′-triOH-BP	7.4 ± 1.2	93 ± 10*	112 ± 9.0*	6.5 ± 1.1	0.099 ± 0.020*

Castrated male F344 rats were treated with T (0.5 mg·kg^{-1}·day^{-1}) and/or MPP (25 mg·kg^{-1}·day^{-1}), MEP (25 mg·kg^{-1}·day^{-1}), BP (300 mg·kg^{-1}·day^{-1}), Flu (6 mg·kg^{-1}·day^{-1}) for a week. Values are mean ± S.E.M. (n = 6), $^{*}p < 0.05$, $^{**}p < 0.01$ *vs.* T. Abbreviations: T, testosterone propionate; Flu, flutamide; MPP, fenthion; MEP, fenitrothion; 2,4,4′-triOH-BP, 2,4,4′-trihydroxybenzophenone.

responsive genes, we carried out quantitative analysis of mRNA expression of three genes in the VP and two in the DP. All of these genes have been reported to be androgen-responsive.[11]

In the VP, expression levels of the kallikrein S3, CRP-1 and prostatein C3 genes in castrated rats were all significantly increased by administration of testosterone (Table 2), while coadministration of flutamide essentially abrogated the effect of testosterone. Coadministration of fenthion had little effect on the action of testosterone, while coadministration of fenitrothion significantly decreased the testosterone-induced increase of kallikrein S3 mRNA. Coadministration of 2,4,4′-triOH-BP significantly enhanced the testosterone-induced increases of CRP-1 and prostatein C3 mRNAs.

In the DP, testosterone increased the expression of PSP94 mRNA, but had no effect on SCGF mRNA, while coadministration of flutamide did not significantly alter the effect of testosterone. Coadministration of fenthion further increased the testosterone-induced expression of PSP94 mRNA, while coadministration of fenitrothion had no effect. Coadministration of 2,4,4′-triOH-BP with testosterone resulted in a significant increase of SCGF mRNA compared with the testosterone-alone group.

DISCUSSION

The Hershberger assay is widely used to study the androgenic and antiandrogenic activity of environmental chemicals. Usually rat prostate is used for this assay. Rat prostate consists of four separate lobes, and although the LP and DP are considered to be homologous to the peripheral zone of human prostate and the AP is similar to the central zone, the VP has no homologous region in human prostate.[15] However, Hershberger assays generally focus on the VP because of its high sensitivity to androgen ablation and to testosterone supplementation after castration. Moreover, there are few alternatives to the Hershberger assay to assess androgenic/antiandrogenic activity *in vivo*. In this study, we assessed the antiandrogenic activities of some known environmental antiandrogens using androgen-responsive genes expressed in the VP and DP as markers. Fenthion and fenitrothion are organophosphorus insecticides; both have been reported to have antiandrogenic activity *in vivo* in the Hershberger assay.[4,12] 2,4,4′-TriOH-BP, a derivative of benzophenone-3 used in sunscreen for humans, is also an antiandrogen.[13] Kallikrein S3, CRP-1 and prostatein C3 are secreted proteins ex-

pressed abundantly in the VP and regulated by androgen.[16–18] We reported that expression of the mRNAs encoding these proteins was increased 10- to 1000-fold in the VP within 24 hr after testosterone treatment in castrated rats.[11] In this study, all the mRNA levels were confirmed to be greatly increased by testosterone and this increase was blocked by co-treatment with flutamide (Table 2). Although fenthion and fenitrothion have been reported to be antiandrogens *in vivo*, we found that they had no effect on the testosterone-induced increases of gene expression in the VP, except for a modest, but significant, decrease of the testosterone-induced increase of kallikrein S3 mRNA by fenitrothion. The reason for this may be the effect of metabolism *in vivo*. Flutamide is converted to hydroxyflutamide, with an increase of about 50-fold in antagonistic activity, while fenthion is inactivated.[12, 19] On the other hand, coadministration of 2,4,4′-triOH-BP enhanced the testosterone-induced increase in the expression of CRP-1 and prostatein C3 in the VP (Table 2).

PSP94 is one of the secreted proteins abundantly expressed in DP.[20] Expression of PSP94 was reportedly increased about 2-fold in the DP in castrated rats after testosterone treatment for 24 hr.[11] In this study, testosterone treatment increased PSP94 mRNA, but flutamide did not block this increase. Fenthion significantly enhanced the testosterone-induced increase of PSP94 mRNA, but fenitrothion and 2,4,4′-triOH-BP were ineffective. SCGF is one of the growth factors expressed in rat prostate, and is expressed highly in the DP. It is tightly regulated by androgen in the DP, being up-regulated about 5-fold within 1 hr after testosterone treatment.[11] In this study, however testosterone did not significantly increase the mRNA level of SCGF, while coadministration of 2,4,4′-triOH-BP resulted in a significant increase compared with testosterone alone (Table 2). The reason for this may be the estrogenicity of 2,4,4′-triOH-BP, which acts as an estrogen agonist in MCF-7 human breast cancer cells and ovariectomized rats.[13, 21] In the rat, estrogen receptor β (ERβ) is expressed in the prostate, and has a role in prostate growth.[22, 23] Its presence may influence the antiandrogenic activity of environmental chemicals. There are differences in response to fenthion, fenitrothion and flutamide between three genes in the VP and two genes in the DP. The reason for this may be the difference in response to testosterone; expression of three genes in the VP greatly increased, on the other hand two genes in the DP did not show great change.

In conclusion, the effects of environmental chemicals on the prostate are very complex, and the Hershberger assay alone appears to be inadequate to understand them. Androgen-responsive genes especially three genes in the VP may be good markers for assessment of androgenic/antiandrogenic activity of environmental chemicals.

REFERENCES

1) Sonnenschein, C. and Soto, A. M. (1998) An updated review of environmental estrogen and androgen mimics and antagonists. *J. Steroid Biochem. Mol. Biol.*, **65**, 143–150.
2) Kim, H. S., Han, S. Y., Yoo, S. D., Lee, B. M. and Park, K. L. (2001) Potential estrogenic effects of bisphenol-A estimated by in vitro and in vivo combination assays. *J. Toxicol. Sci.*, **26**, 111–118.
3) Kelce, W. R., Stone, C. R., Laws, S. C., Gray, L. E., Kemppainen, J. A. and Wilson, E. M. (1995) Persistent DDT metabolite p,p′-DDE is a potent androgen receptor antagonist. *Nature*, **375**, 581–585.
4) Tamura, H., Maness, S. C., Reischmann, K., Dorman, D. C., Gray, L. E. and Gaido, K. W. (2001) Androgen receptor antagonism by the organophosphate insecticide fenitrothion. *Toxicol. Sci.*, **60**, 56–62.
5) Gray, Jr. L. E. (1998) Tiered screening and testing strategy for xenoestrogens and antiandrogens. *Toxicol. Lett.*, **102–103**, 677–680.
6) O'Connor, J. C., Frame, S. R., Davis, L. G. and Cook, J. C. (1999) Detection of the environmental antiandrogen p,p-DDE in CD and long-evans rats using a tier I screening battery and a Hershberger assay. *Toxicol. Sci.*, **51**, 44–53.
7) Ashby, J. and Lefevre, P. A. (2000) The peripubertal male rat assay as an alternative to the Hershberger castrated male rat assay for the detection of antiandrogens, oestrogens and metabolic modulators. *J. Appl. Toxicol.*, **20**, 35–47.
8) Hershberger, L. G., Shipley, E. G. and Meyer, R. K. (1953) Myotrophic activity of 19-nortestosterone and other steroids determined by modified levator ani muscle method. *Proc. Soc. Exp. Biol. Med.*, **83**, 175–180.
9) EDSTAC (1998) Endocrine Disruptor Screening and Testing Adversory Committee (EDSTAC) Final Report. US Environmental Protection Agency.
10) Hayashi, N., Sugimura, Y., Kawamura, J., Donjacour, A. A. and Cunha, G. R. (1991) Morphological and functional heterogeneity in the rat prostatic

gland. *Biol. Reprod.*, **45**, 308-321.
11) Suzuki, T., Fujimoto, N., Kitamura, S. and Ohta, S. (2007) Quantitative determination of lobe specificity of mRNA expression of androgen-dependent genes in the rat prostate gland. *Endocr. J.*, **54**, 123–132.
12) Kitamura, S., Suzuki, T., Ohta, S. and Fujimoto, N. (2003) Antiandrogenic activity and metabolism of the organophosphorus pesticide fenthion and related compounds. *Environ. Health Perspect.*, **111**, 503–508.
13) Suzuki, T., Kitamura, S., Khota, R., Sugihara, K., Fujimoto, N. and Ohta, S. (2005) Estrogenic and antiandrogenic activities of 17 benzophenone derivatives used as UV stabilizers and sunscreens. *Toxicol. Appl Pharmacol.*, **203**, 9–17.
14) Woo, T. H., Patel, B. K., Cinco, M., Smythe, L. D., Symonds, M. L., Norris, M. A. and Dohnt, M. F. (1998) Real-time homogeneous assay of rapid cycle polymerase chain reaction product for identification of Leptonema illini. *Anal. Biochem.*, **259**, 112–117.
15) Cunha, G. R., Donjacour, A. A., Cooke, P. S., Mee, S., Bigsby, R. M., Higgins, S. J. and Sugimura, Y. (1987) The endocrinology and developmental biology of the prostate. *Endocr. Rev.*, **8**, 338–362.
16) Clements, J. A., Matheson, B. A., Wines, D. R., Brady, J. M., MacDonald, R. J. and Funder, J. W. (1988) Androgen dependence of specific kallikrein gene family members expressed in rat prostate. *J. Biol. Chem.*, **263**, 16132–16137.
17) Heyns, W. (1990) Androgen-regulated proteins in the rat ventral prostate. *Andrologia*, **22 Suppl 1**, 67–73.
18) Vercaeren, I., Vanaken, H., Devos, A., Peeters, B., Verhoeven, G. and Heyns, W. (1996) Androgens transcriptionally regulate the expression of cystatin-related protein and the C3 component of prostatic binding protein in rat ventral prostate and lacrimal gland. *Endocrinology*, **137**, 4713–4720.
19) Kelce, W. R., Monosson, E., Gamcsik, M. P., Laws, S. C. and Gray, L. E. (1994) Environmental hormone disruptors: evidence that vinclozolin developmental toxicity is mediated by antiandrogenic metabolites. *Toxicol. Appl. Pharmacol.*, **126**, 276–285.
20) Kwong, J., Xuan, J. W., Chan, P. S., Ho, S. M. and Chan, F. L. (2000) A comparative study of hormonal regulation of three secretory proteins (prostatic secretory protein-PSP94, probasin, and seminal vesicle secretion II) in rat lateral prostate. *Endocrinology*, **141**, 4543–4551.
21) Yamasaki, K., Takeyoshim, M., Sawaki, M., Imatanaka, N., Shinoda, K. and Takatsuki, M. (2003) Immature rat uterotrophic assay of 18 chemicals and Hershberger assay of 30 chemicals. *Toxicology*, **183**, 93–115.
22) Horvath, L. G., Henshall, S. M., Lee, C. S., Head, D. R., Quinn, D. I., Makela, S., Delprado, W., Golovsky, D., Brenner, P. C., O'Neill, G., Kooner, R., Stricker, P. D., Grygiel, J. J., Gustafsson, J. A. and Sutherland, R. L. (2001) Frequent loss of estrogen receptor-beta expression in prostate cancer. *Cancer Res.*, **61**, 5331–5335.
23) Weihua, Z., Makela, S., Andersson, L. C., Salmi, S., Saji, S., Webster, J. I., Jensen, E. V., Nilsson, S., Warner, M. and Gustafsson, J. A. (2001) A role for estrogen receptor beta in the regulation of growth of the ventral prostate. *Proc. Natl. Acad. Sci. U.S.A.*, **98**, 6330–6335.

Hypothalamus Region-Specific Global Gene Expression Profiling in Early Stages of Central Endocrine Disruption in Rat Neonates Injected with Estradiol Benzoate or Flutamide

Makoto Shibutani,[1] Kyoung-Youl Lee,[1]* Katsuhide Igarashi,[2] Gye-Hyeong Woo,[1] Kaoru Inoue,[1] Tetsuji Nishimura,[3] Masao Hirose[1]

[1] Division of Pathology, National Institute of Health Sciences, Setagaya-ku, Tokyo 158-8501, Japan

[2] Division of Molecular Toxicology, National Institute of Health Sciences, Setagaya-ku, Tokyo 158-8501, Japan

[3] Division of Environmental Chemistry, National Institute of Health Sciences, Setagaya-ku, Tokyo 158-8501, Japan

Received 3 February 2006; revised 8 September 2006; accepted 14 September 2006

ABSTRACT: To identify genes linked to early stages of disruption of brain sexual differentiation, hypothalamic region-specific microarray analyses were performed using a microdissection technique with neonatal rats exposed to endocrine-acting drugs. To validate the methodology, the expression fidelity of microarrays was first examined with two-round amplified antisense RNAs (aRNAs) from methacarn-fixed paraffin-embedded tissue (PET) in comparison with expression in unfixed frozen tissue (UFT). Decline of expression fidelity when compared with the 1×-amplified aRNAs from UFTs was found as a result of the preferential amplification of the 3′ side of mRNAs in the second round *in vitro* transcription. However, expression patterns for the 2×-amplified aRNAs were mostly identical between methacarn-fixed PET and UFT, suggesting no obvious influence of methacarn fixation and subsequent paraffin embedding on expression levels. Next, in the main experiment, neonatal rats at birth were treated subcutaneously either with estradiol benzoate (EB; 10 μg/pup) or flutamide (FA; 250 μg/pup), and medial preoptic area (MPOA)-specific microarray analysis was performed 24 h later using 2×-amplified aRNAs from methacarn-fixed PET. Numbers of genes showing constitutively high expression in the MPOA predominated in males, implying a link with male-type growth supported by perinatal testosterone. Around 60% of genes showing sex differences in expression demonstrated altered levels after EB treatment in females, suggesting an involvement of genes necessary for brain sexual differentiation. When compared with EB, FA affected a rather small number of genes, but fluctuation was mostly observed in females, as with EB. Moreover, many selected genes common to EB and FA showed down-regulation in females with both drugs, suggesting a common mechanism for endocrine center disruption in females, at least at early stages of post-natal development. Develop Neurobiol 67: 253–269, 2007

Keywords: brain sexual differentiation; microarray; estradiol benzoate; flutamide; microdissection

INTRODUCTION

Sex steroids play important roles in sexual differentiation of the mammalian brain (McEwen and Alves, 1999). In the rat, there is a critical period beginning

*Present address: Toxicological Research Team, Occupational Safety and Health Research Institute, 104-8, Munji-Dong, Yuseong-Gu, Daejeon, 305-380, Korea.

Correspondence to: M. Shibutani (shibutan@nihs.go.jp).

Contract grant sponsors: Ministry of the Environment, Ministry of Health, Labor and Welfare of Japan.

Published online 3 January 2007 in Wiley InterScience (www.interscience.wiley.com).
DOI 10.1002/dneu.20349

at the last week of gestation and terminating in few days after birth, during which circulating testosterone secreted from the fetal and neonatal testes masculinizes the brain in males (Rhees et al., 1990a,b), the hormone being metabolized to estradiol by the enzyme aromatase to trigger brain sexual differentiation. Steroid-mediated processes during this period, including alterations in neuronal plasticity, myelination, and cell death, are the basis of sexual dimorphism in the structure and function of the adult brain (Matsumoto et al., 2000). For example, the medial preoptic area (MPOA) in the hypothalamus that is believed to mediate sexually dimorphic behavior in adult life (Meisel and Sachs, 1994; Numan, 1994) contains a highly cellular region, the sexually dimorphic nucleus of preoptic area (SDN-POA), that has an approximately 10 times larger volume in males than in females (Meredith et al., 2001). Inhibitory effects of steroids against the normal apoptosis that proceeds in the female SDN-POA during the critical period have been suggested to be responsible for the large size in males (Arai et al., 1996; Davis et al., 1996).

Sex steroids with their receptors are powerful regulators of gene transcription, and changes in the hormonal milieu during development can trigger reproductive dysfunction in later life by affecting molecular cascades responsible for sexual differentiation (McEwen and Alves, 1999). For instance, both α and β estrogen receptors (ERs) are strongly expressed in the hypothalamus during neonatal development, showing region-specific distributions (Orikasa et al., 2002), and neonatal hormonal manipulations can affect their expression levels and/or locations (Tena-Sempere et al., 2001; Orikasa et al., 2002), resulting in organizational changes in the brain structure and reproductive function in later life (Nagao et al., 1999; Tsukahara et al., 2003).

To elucidate mechanisms underlying disruption of brain sexual differentiation, gene screening applying global gene expression profiling in target brain region(s) is an effective approach. We recently established multipurpose genetic analysis methods with paraffin-embedded tissues (PETs) utilizing methacarn as a novel fixation tool, in combination with laser microbeam microdissection (Shibutani et al., 2000; Shibutani and Uneyama, 2002; Uneyama et al., 2002). With this system, we could achieve high performance regarding quantitative expression analysis of mRNAs using real-time RT-PCR, close to that with unfixed frozen tissue (UFT) (Takagi et al., 2004).

In the present study, we focused on region-specific gene expression analysis utilizing microarrays to identify genes linked with disruption of brain sexual differentiation in rats. With limited tissue samples, such as those collected by microdissection, multi-round amplification of mRNAs is necessary to obtain sufficient quantities of antisense RNAs (aRNAs) applicable for microarray analysis, and therefore, we first performed validation experiments using methacarn-fixed liver PETs to determine fidelity of expression profiles with 2× *in vitro* transcribed aRNAs in comparison with 1×- or 2×-amplified examples from UFTs. After confirmation of the efficacy of the methods, we then analyzed gene expression profiles in the neonatal MPOA in terms of sex differences and acute responses to neonatally injected estradiol benzoate (EB), a potent analog of endogenous estrogen, or flutamide (FA), a non-steroidal anti-androgen.

METHODS

Chemicals and Animals

Estradiol benzoate (EB; CAS# 50-50-0) and flutamide (FA; CAS# 13311-84-7) were purchased from Sigma (St. Louis, MO), sodium phenobarbital (PB; CAS# 57-30-7) from Wako Pure Chemical Industries (Osaka, Japan) and CD^{R}(SD)IGS rats from Charles River Japan (Kanagawa, Japan). For the preliminary validation study regarding expression fidelity with microarrays using methacarn-fixed PET, one 7-week-old male rat was used, and for gene expression profiling in the early stage of disruption of brain sexual differentiation, six pregnant rats at gestational Day 3 (the day when vaginal plugs were observed was designated as GD 0). The animals were housed individually in polycarbonate cages (SK-Clean, 41.5 × 26 × 17.5 cm in size; CLEA Japan, Tokyo) with wood bedding (Soft Chip; Sankyo Lab Service, Tokyo, Japan), maintained in an air-conditioned animal room (temperature: 24°C ± 1°C, relative humidity: 55% ± 5%) with a 12-h light–dark cycle, and allowed *ad libitum* access to feed and tap water. For the rat in the preliminary validation study, CRF-1, a standard rodent diet, purchased from Oriental Yeast Co. (Tokyo, Japan), was used as the basal diet. For pregnant animals, soy-free diet (Oriental Yeast Co.) was used as a basal diet to remove possible interaction of phytoestrogens included in the regular soy-containing diet with the action of EB or FA. The formulation of the soy-free diet as well as the dietary concentrations of estrogens and phytoestrogens were as described earlier (Masutomi et al., 2003). Essentially, concentrations of phytoestrogens except for coumestrol, detected at 0.3 mg/100 g diet, were lower than the detection limit (0.05 mg/100 g diet).

Experimental Design

In the preliminary validation study, the rat received PB intraperitoneally at 80 mg/kg, once daily for three days. The dose was selected according to the PB-specific enzyme

induction protocol described by Kocarek et al. (1998). One day after the last injection, the animal was killed by exsanguination from the abdominal aorta under ether anesthesia, and the liver was removed and trimmed to make tissue blocks sized 5 × 5 × 3 mm.

For gene expression profiling in the early stage of disruption of brain sexual differentiation, offspring of two dams each were injected subcutaneously either with EB, FA, or vehicle at postnatal day (PND) 1 (the day of delivery) within 3–6 h after completion of delivery. The dose level of EB was set as 10 μg/pup, shown in our laboratory, to induce typical estrogenic effects on sexual development and the endocrine/reproductive system at the adult stage in both sexes, including reduction of the SDN volume in males (Shibutani et al., 2005). For FA, 250 μg/pup was selected on the basis of earlier study finding of retardation of male reproductive development with repeated injections of this dose (Rivas et al., 2002). Each chemical was dissolved in sesame oil to achieve a total injection volume of 20 μL. Vehicle control animals were injected with 20 μL of sesame oil. Twenty-four hours after the injection (PND 2), offspring including vehicle control pups were killed by decapitation for removal of brains.

The animal protocols were reviewed and approved by the Animal Care and Use Committee of the National Institute of Health Sciences, Japan.

Preparation of Tissue Specimens and Microdissection

Liver tissues of the rat treated with PB were either quick frozen in ethanol–dry ice after embedding in Tissue-Tek 4583 OCT compound (Sakura Finetek Japan, Tokyo, Japan), or immersed in methacarn for tissue fixation. For this purpose, methacarn solution consisting of 60% (vol/vol) absolute methanol, 30% chloroform, and 10% glacial acetic acid was freshly prepared and stored at 4°C (Shibutani et al., 2000; Shibutani and Uneyama, 2002; Takagi et al., 2004), before fixation for 2 h at 4°C. Fixed tissue samples were then dehydrated three times for 1 h in fresh 99.5% ethanol at 4°C, immersed in xylene once for 1 h and then three times for 30 min at room temperature, and immersed in hot paraffin (60°C) four times for 1 h, for a total of 4 h. Both UFTs (n = 3) and methacarn-fixed PETs (n = 3) were sectioned at 10 μm and 20 sections per block were stored in 1.5 mL tubes at −80°C until RNA extraction.

For MPOA-specific microarray analysis, whole brains of rat pups were subjected to methacarn fixation (n = 3/sex/group). Before embedding, coronal brain slices including the hypothalamus were trimmed. Microdissection of the MPOA was performed based on the method described earlier (Takagi et al., 2004). After paraffin embedding, 6-μm-thick sections between three 18-μm-thick sections were prepared. The 18-μm sections were mounted onto PEN-foil film (Leica Microsystems, Tokyo, Japan) overlaid on glass slides, dried in an incubator overnight at 37°C, deparaffinized with xylene three times each for 3 min, placed in 99.5% ethanol for 1 min, and then air-dried. The localization of the SDN-POA, identified as an intensely stained cellular region, was determined by microscopic observation of the 6-μm-thick sections stained with hematoxylin and eosin (HE) (as shown in Fig. 1), and bilateral portions of the MPOA (500 × 300 μm) containing SDN-POA were microdissected from the adjacent unstained 18-μm-thick sections using PALM Robot-MicroBeam equipment (Carl Zeiss Co., Tokyo, Japan). In both sexes, 10–12 sections from one animal were used for microdissection, and the microdissected samples were stored in one 1.5 mL sample tube at −80°C until extraction of total RNA.

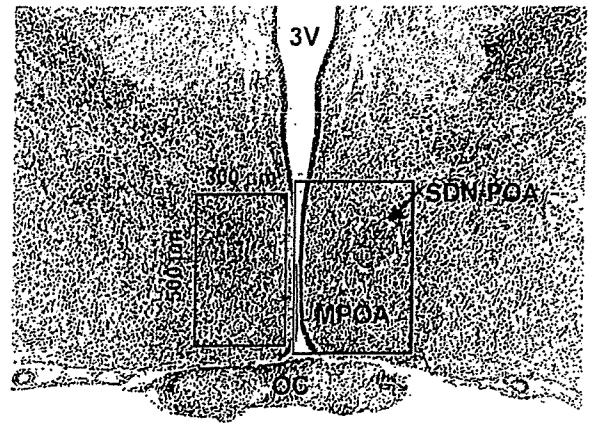

Figure 1 Overview of the hypothalamic MPOA at PND 2. Bilateral portions of MPOA as shown in the left boxed area were microdissected from sections of methacarn-fixed paraffin-embedded brain slices for gene expression analysis. The right boxed area is the anatomical location for immunohistochemical observation of protein signals shown in Table 6 and Fig. 6 (3V, third ventricle; SDN-POA, sexually dimorphic nucleus of the preoptic area; MPOA, medial preoptic area; OC, optic chiasm).

RNA Isolation, Amplification, and Microarray Analysis

Total RNAs from liver sections of UFTs and methacarn-fixed PETs were extracted with RNeasy® Mini (QIAGEN, Hilden, Germany) according to the manufacturer's protocol, with the final elution volume set at 30 μL. Contaminating genomic DNA was digested with DNase I (Ambion, Austin, TX) at the end of the extraction. Total RNAs from microdissected MPOAs were extracted using an RNAquous®-Micro RNA isolation kit (Ambion), eluted twice with a total volume of 14 μL, and then treated with DNase according to the manufacturer's protocol.

For quantitation of RNA yield, 1 μL of isolated RNA was labeled with a RiboGreen™ RNA Quantitation kit (Molecular Probes, Eugene, Oregon) and concentrations were estimated with a fluorescence spectrophotometer F2500 (Hitachi Co., Tokyo, Japan) in 1 mL of total volume with water.

For microarray analysis, extracted total RNA samples were subjected to amplification, consisting of reverse tran-

scription and subsequent *in vitro* transcription, using a MessageAmp™ aRNA Kit (Ambion) with an oligo dT/T7 primer, according to the manufacturer's protocol. Total RNA samples from liver UFT sections were either subjected to one- or two-step amplification, and those from methacarn-fixed liver PET sections were subjected to two-step amplification. For expression analysis with the microdissected MPOA, two-step amplification was performed. For one-step amplification, 5 μg of total RNA was subjected to one-round of aRNA amplification. For the two-step amplification, 50 ng of total RNA was subjected to first-round amplification, and resultant aRNAs of 150–200 ng were subjected to second-round amplification. During the second *in vitro* transcription, generating aRNAs were labeled with biotin-UTP and biotin-CTP (Enzo Biochem, Farmingdale, NY).

For normalization of transcript levels with reference to amplification efficiency, an *in vitro* transcribed spike RNA from pGIBS-PHE (American Type Culture Collection, Manassas, VA), a short fragment of *Bacillus subtilis* (accession no. M24537 in GenBank/EMBL data bank), was added to the extracted total RNA at 3.76 pg/μg.

After the second-round amplification, 20 μg of biotinylated aRNA was denatured at 94°C for 35 min in fragmentation buffer (4×10^{-2} *M* Tris-acetate, pH 8.1, 1×10^{-7} *M* KOAc, 3×10^{-2} *M* MgOAc) and subjected to hybridization in a mixture containing control cRNAs (Affymetrix, Santa Clara, CA). Aliquots of 200 μL containing approximately 15 μg of aRNA were hybridized with GeneChip® Rat Genome U34A Arrays (Affymetrix) at 45°C for 18 h, stained with streptavidin/R-phycoerythrin conjugates (Molecular Probes), and then scanned with a GeneChip® Scanner 3000 (Affymetrix). Individual samples were subjected to analysis with individual microarrays in both the validation study and the MPOA-specific gene expression profiling study (n = 3/group for comparison in each study).

Real-Time RT-PCR

Quantitative real-time RT-PCR was performed for confirmation of expression values obtained with microarrays using ABI Prism 7700 (Applied Biosystems Japan, Tokyo, Japan). In a separate microarray study, to investigate gene expression changes in microdissected MPOA of rat neonates that have been administered 0.01–0.5 ppm ethinylestradiol through the maternal diet, we selected two genes, i.e., thymosin β4 and GTP-binding protein (Gαi2), showing profound sex differences in basal expression. Gene specific primers for thymosin β4 (accession no. NM_031136 in the GenBank/EMBL data banks) and Gαi2 (M12672) as well as corresponding TaqMan® MGB probes (6-FAM™-dye-labeled) were obtained from Assays-on-Demand™ Gene Expression Products (Applied Biosystems Japan). Reverse transcription was performed using 100 ng of first-round aRNAs prepared for microarray analysis containing spike RNA with a high-capacity cDNA Archive Kit (Applied Biosystems Japan) in a 100 μL total reaction volume. Real-time PCR was performed in a 50 μL reaction volume using the TaqMan probe detection system with 25 μL of TaqMan® Universal PCR Master Mix (Applied Biosystems Japan) and 2.5 μL each of target primer mix and RT product. Cycle parameters with this system were: single step of 50°C for 2 min, initial activation at 95°C for 10 min, 45 cycles of 15 sec at 95°C, and 60 sec at 60°C. For quantitation of expression data, a standard curve method was applied using first-round amplified aRNAs from a male MPOA as a standard sample.

For the spike gene (*Bacillus subtilis*), *in vitro* amplified transcript levels were measured by one-step real-time RT-PCR using the SYBR® Green detection system in a 50 μL total reaction mixture containing 25 μL of 2× QuantiTect™ SYBR® Green PCR Master Mix (QIAGEN), 8 ng of first-round amplified aRNA, multiscribe RTase (17.5 units), RNase inhibitor (20 units), and 2.5×10^{-7} *M* of primers. Cycle parameters in this system were as follows: 48°C for 30 min, 95°C for 10 min, 45 cycles of 15 sec at 95°C, and 60 sec at 60°C. The primer set for the spike gene, 5′-AGCGCCCCGGACTGA-3′ (forward; nucleotides 3152–3166), and 5′-CTCTAGGCCCAAAACGACCTT-3′ (reverse; nucleotides 3107–3127), was designed using Primer Express® software (Version 2.0; Applied Biosystems Japan).

Immunohistochemical Analysis

Whole brains of male and female neonates injected with EB or vehicle at PND 1 and obtained on PND 2 were subjected to fixation in Bouin's solution overnight (n = 4/sex/group). Coronal brain slices including the hypothalamus were trimmed and paraffin-embedded, and 3-μm serial sections were prepared for localization of the MPOA including the SDN-POA with HE-stained sections each one prepared in every 10 sections.

Immunohistochemistry was performed with antibodies against poly(ADP-ribose) polymerase (PARP) (rabbit IgG, 50× dilution; Santa Cruz Biotechnology, Santa Cruz, CA), glutamate receptor (GluR) 1 (rabbit immunoaffinity purified IgG, 1 μg/mL; Upstate, Charlottesville, VA), GluR5 (rabbit polyclonal IgG, 100× dilution; Upstate), GluR6/7 (rabbit immunoaffinity purified IgG, 5 μg/mL; Upstate), microtubule-associated protein (MAP) 2 (mouse monoclonal IgG_1, 400× dilution; Chemicon International, Inc, Temecula, CA), and metallothionein-1/2 (MT-1/2; clone E9, mouse $IgG_{1,\kappa}$, 400× dilution; DakoCytomation, Carpinteria, CA). The PARP antibody can detect PARP-1, and to a lesser extent PARP-2, according to the manufacturer's product information. For detection of GluR1, GluR5, and GluR6/7, deparaffinized sections were subjected to microwave treatment, four times for 3 min in 1×10^{-2} *M* citrate buffer (pH 6.0), according to the recommendation in the manufacturer's protocol. For MAP2, microwave treatment was performed twice for 3 min in the same citrate buffer. Nonspecific endogenous peroxidase activity was blocked by treatment with 0.9% hydrogen peroxide in absolute methanol for 10 min. After masking with normal goat (for rabbit polyclonal antibodies) or horse (for mouse monoclonal antibod-

Table 1 Comparison of the Expression Status of Genes in Microarrays Between aRNA Samples Prepared from UFT and Methacarn-Fixed PET[a]

Tissue Status	UFT		Methacarn-Fixed PET
aRNA Sample	1× amplified	2× amplified	2× amplified
Rates with gene probes for each expression status (%)			
Present	40.3	36.9	36.4
Absent	57.5	60.9	61.5
Marginal	2.2	2.2	2.1
Signal ratio with the GAPDH gene (3′/5′, × fold)	1.1	12.3	11.3

aRNA, antisense RNA; UFT, unfixed frozen tissue; PET, paraffin-embedded tissue; GAPDH, glyceraldehyde-3-phosphate dehydrogenase.
[a]Liver tissue of a rat treated daily with sodium phenobarbital (80 mg/kg body weight, s.c.) for three days was used.

ies) serum, sections were incubated with primary antibodies, overnight at 4°C, and subsequently with biotinylated secondary antibody for 60 min at room temperature. All antibodies used were diluted with 0.5% casein in PBS before application. Immunodetection was carried out with the horseradish peroxidase–avidin–biotin complex utilizing a VECTASTAIN® Elite ABC kit (Vector Laboratories, Burlingame, CA), with 3,3′-diaminobenzidine/H_2O_2 as the chromogen. Sections were counterstained with hematoxylin for microscopic examination. For quantitative measurement of the numbers of nuclei immunoreactive for PARP, bilateral portions of a 250 × 250 μm area covering the SDN region were subjected to analysis under 200× magnification. Also, nuclei immunoreactive for MT-1/2 were counted in bilateral MPOAs by randomly selecting three fields (125 × 125 μm area) on each side under 400× magnification. For each antigen (PARP and MT-1/2), mean ratios of nuclear immunoreactive cells to the total cells counted in each side were estimated.

Data Analysis

Scanned output files of microarrays were visually inspected for hybridization artifacts, and then expression signals for each gene were measured by calculating pixel intensities using a Microarray Suite software package (Version 5.0, Affymetrix). With this software, the expression status of each gene, whether present, absent, or marginally expressed, was judged. Exclusion of genes showing absence in at least three of six samples of the two groups for comparison of expression, normalization of expression data, and statistical comparisons were performed using GeneSpring® software (Version 5; Silicon Genetics; Redwood City, CA). For microarray data in the validation study of expression fidelity with methacarn-fixed PET specimens, per chip normalization was performed by dividing the signal strength for each gene with the level of the 50th percentile of the measurement in the chip, and per gene normalization with average signal strength of the identical gene of three 1×-amplified aRNAs samples from UFTs. With regard to the microarray data for microdissected MPOA, per chip normalization was performed by dividing the signal strength of each gene by the level of the spike RNA signal in each sample, and per gene normalization with average signal strength of the identical gene in three untreated control samples. Average relative expression values were determined for each gene in the treatment group, and genes showing expression changes with ≥2-fold differences were first estimated. Then, comparison of expression data between the untreated controls and each treatment group was performed using Student's *t*-test with multiple testing corrections applying Benjamini and Hochberg false positive discovery rate calculations, and genes showing statistical significance with a p value <0.05 were selected.

To assess fidelity of expression patterns in microarrays between the 2×-amplified aRNA samples from methacarn-fixed liver PETs and 1×- and 2×-amplified samples from liver UFTs, Pearson's correlation coefficients (r) for each combination were estimated using all genes included in the array.

For the real-time RT-PCR data, expression values were normalized to the amplification efficiency of the first-round *in vitro* transcription by dividing the expression values with the signal level of spike RNA included in each sample. Differences in expression levels between sexes were analyzed by the Student's *t*-test, when the variance proved to be homogeneous among groups using the test for equal variance. If a significant difference in the variance was observed, a Welch's *t*-test was performed.

Morphometrically analyzed data for nuclear immunoreactive cell ratios of PARP and MT-1/2 were compared by Student's and Welch's *t*-tests. Regarding immunoreactivities on which morphometric analysis could not be applied, total incidence of immunoreactive cases and grades of intensity were visually analyzed and statistically compared using the Fisher's exact probability test and Mann–Whitney's *U*-test, respectively.

RESULTS

Expression Fidelity in Methacarn-fixed PETs

Expression fidelity of the microdissected small tissue samples in microarray analysis might be influenced by tissue processing for microdissection and/or multiround amplification. To clarify the effect of tissue processing for microdissection (methacarn-fixation and following paraffin-embedding) on the expression

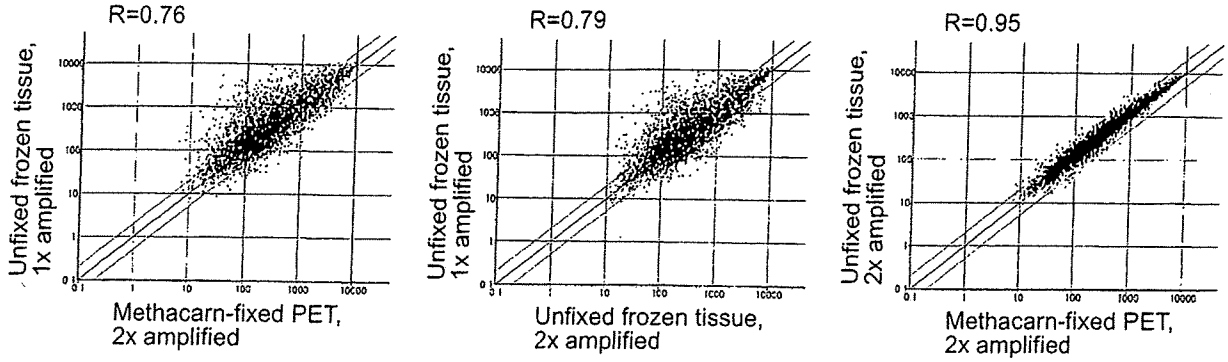

Figure 2 Scatter plot analysis of gene expression profiles of aRNA samples derived from methacarn-fixed PET and UFT of rat liver.

fidelity after 2×-amplification, expression in the second-round amplified aRNA samples was compared with that obtained from the 1×- or 2×-amplified aRNAs from UFT. With the 8799 probes included in the array used, percentages of expression status (present, absent, and marginal) were similar among aRNA-preparations irrespective of the tissue status and the amplification cycle (Table 1). However, preferential amplification of the 3′ portions was evident with 2× amplification in both UFT and methacarn-fixed PET cases (Table 1). By scatter plot analysis, high correlations were observed in the expression profiles between the 2×-amplified aRNAs from methacarn-fixed PET and UFT ($r = 0.95$, $n = 3$; Fig. 2). When the correlation of gene expression levels was examined between the 1×-amplified aRNAs from UFT and 2×-amplified ones from either methacarn-fixed PET or UFT, r values were similar, but relatively low when compared with the value for the correlation between the two 2× amplified examples, indicating a lowered expression fidelity in the methacarn-fixed PET because of the second-round amplification. When the number of genes showing presence was examined for 2×-amplified methacarn-fixed PET and 1×-amplified UFT aRNAs, 3173 probes were positive in common (as shown in Fig. 3). The numbers of probes showing presence solely in the methacarn-fixed PET (2× amplified) and UFT (1× amplified) were 373 and 822, respectively, suggesting that 10.5% of the total genes exhibiting presence in the 2×-amplified samples should be regarded to be false positive, and that 20.6% of the present genes in the 1×-amplified samples from UFT lost their signals after two-round amplification. It is possible that the distance from the poly(A) tail to the positions of the probes may affect the expression status of each gene after the second-round *in vitro* transcription due to preferential amplification of the 3′-terminal portion. Among genes showing presence solely in the methacarn-fixed PET (2× amplified) and UFT (1× amplified), sequence information including the full 3′-untranslated region from the poly(A) tail was available for six and five genes, respectively. The mean distances from the 5′-end of the probes (both 5′- and 3′-most probes) to the 5′-end of poly(A) tail expressed as the number of nucleotides were examined for these (Table 2), and as expected, they were shorter with 2×-amplified aRNA samples from methacarn-fixed PET than with their 1×-amplified counterparts from UFT. These results indicate that the decline in expression fidelity with 2×-amplified samples is mainly due to preferential amplification at the 3′-portions by the second-round amplification and methacarn fixation and paraffin-embedding did not apparently affect the fidelity.

Gene Expression Profiles of MPOA of Neonates Acutely Treated with EB or FA

In the MPOAs at PND 2, about 3600 genes showed presence in both sexes in untreated controls. Sex dif-

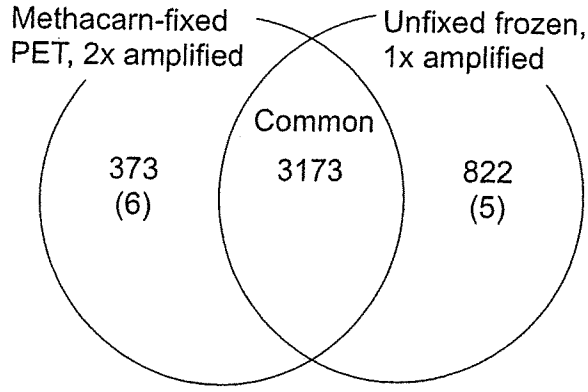

Figure 3 Gene populations showing presence with aRNA samples 2×-amplified from methacarn-fixed PET and 1×-amplified from UFT.